Physics – Uspekhi **63** (2) 145 – 161 (2020)

REVIEWS OF TOPICAL PROBLEMS PACS numbers: 05.45.Ra, 05.45.Xt, **05.65. + b**

Spatio-temporal structures in ensembles of coupled chaotic systems

G I Strelkova, V S Anishchenko

DOI: https://doi.org/10.3367/UFNe.2019.01.038518

Contents

Abstract. We review numerical results of studies of the complex dynamics of one- and double-dimensional networks (ensembles) of nonlocally coupled identical chaotic oscillators in the form of discrete- and continuous-time systems, as well as lattices of coupled ensembles. We show that these complex networks can demonstrate specific types of spatio-temporal patterns in the form of chimera states, known as the coexistence of spatially localized domains of coherent (synchronized) and incoherent (asynchronous) dynamics in a network of nonlocally coupled identical oscillators. We describe phase, amplitude, and double-well chimeras and solitary states; their basic characteristics are analyzed and compared. We focus on two basic discrete-time models, Hénon and Lozi maps, which can be used to describe typical chimera structures and solitary states in networks of a wide range of chaotic oscillators. We discuss the bifurcation mechanisms of their appearance and evolution. In conclusion, we describe effects of synchronization of chimera states in coupled ensembles of chaotic maps.

Keywords: ensembles, nonlocal coupling, chimera states, spatio-temporal structure, synchronization, discrete maps, dynamical chaos

G I Strelkova (*), **V S Anishchenko** (**)
Chernyshevskii Saratov State University,
ul. Astrakhanskaya 83, 410012 Saratov, Russian Federation
E-mail: (*) strelkovagi@info.sgu.ru, (**) wadim@info.sgu.ru

Received 10 October 2018, revised 10 January 2019
Uspekhi Fizicheskikh Nauk **190** (2) 160 – 178 (2020)
Translated by S D Danilov; edited by A M Semikhatov

1. Introduction

Already over the last several decades, studies of collective dynamics in complex systems of various natures, synchronization in ensembles of coupled oscillators, the formation of various dissipative structures, and their evolution have been one of the central themes of nonlinear dynamics and the related interdisciplinary branches of science. Results collected in these studies are reflected in numerous monographs [1–15] and articles [16–46]. It has been found that structures such as clusters of synchronization, spatial intermittency, regular and chaotic patterns fixed in space can form in nonlinear ensembles and networks. In many studies, as a rule, ensembles of identical oscillatory elements coupled locally or globally have been explored.

Relatively recently, spatio-temporal structures of a new type, called chimera states, were discovered [47, 48]. This discovery was in essence brought about by the introduction of nonlocal coupling between the ensemble elements. A nonlocal coupling implies that each oscillator in the ensemble is connected to a finite number of nearest-neighbor oscillators on the right and left. Such a state was first discovered in a one-dimensional ensemble of nonlinearly coupled identical phase oscillators [47] and then explored in more detail in Ref. [48], where the name *chimera state* or *chimera* was also proposed. The term 'chimera', from Greek mythology, characterizes a combination of the 'compatible' with the 'incompatible'.

We note that structures resembling chimeras were observed long before they were defined in Refs [47, 48]. The attention of researchers in those days was focused on the analysis and control of transitions from regimes of spatial chaos to those when all elements in the ensembles are fully synchronized. Chimera-type structures were observed in the

transition to synchronization regimes and were referred to as synchronous and asynchronous clusters [17, 25].

Over the last few years, studies of chimera structures have been attracting attention, piquing the interest of numerous researchers and leading to a growing number of numerical and theoretical studies [49–98], followed by experimental work [99–107]. It has been shown that the appearance of chimera states is not limited to phase oscillators. Such states are observed in ensembles with partial elements of various types: in discrete-time [55, 56, 66, 75–77, 86–88, 90, 91, 96, 98] and continuous-time [55, 56, 70, 81, 91, 93, 97] chaotic systems, in van der Pol oscillators [79, 81, 84], in excitable systems like the FitzHugh–Nagumo neuron model and other models of neuronal activity [57, 67, 80, 81, 85, 89, 94, 108], in population models [70, 83], and in autonomous Boolean networks [42, 58]. At present, chimera structures are observed in laboratory experiments in optical, optoelectronic, laser [99, 102, 105], chemical [100, 101], and mechanical systems [103, 104]. Work on possible applications of chimera structures to describe the dynamics of ensembles in living nature is in progress. Chimera states are explored in relation to the analysis of alternating sleep phases of brain hemispheres [109, 110], epileptic seizures [111, 112], the activity of brain neurons [113, 115], and cardiac muscle dynamics (fibrillation of ventricles) [116, 117]. Studying chimera states is also of practical importance for the analysis of stable functioning regimes of power grids [118, 119] or transport networks [120], etc.

Very recent research is directed at finding the specifics of chimera states in ensembles of various nonlinear oscillators, attempts to describe their realization mechanisms, and the analysis of the impact of the topology of coupling between ensemble elements [67, 70, 79, 81, 84, 85] and the role of noise perturbations [82, 90, 98, 121]. Attempts have been made to classify the types of chimera structures [78, 91]. We specially stress the important role of specifying initial conditions for individual ensemble oscillators. As a rule, chimera states are explored in ensembles of identical oscillators. Given a symmetric topology of coupling between the elements and identical initial conditions, the ensemble demonstrates synchronous dynamics without forming incoherent clusters. Therefore, initial conditions are either set in a special way in the space of ensemble oscillators or selected as randomly distributed in some interval. The latter way seems to be preferable because it corresponds to the functioning of real ensembles in nature or technology.

In spite of numerous studies exploring chimeras in various ensembles, many questions remain unsolved or have been solved incompletely. Of fundamental importance is the question of chimera state stability. Are the chimeras stable or they are only a long-lasting transient process? Most publications base the conclusion about stability on numerical simulations. However, it should be realized that a numerical experiment is "not in position to distinguish between stable states and long-lived transient processes" [65]. A theoretical stability analysis requires obtaining an analytic solution for the regime of the chimera ensemble state. This problem has been unsolvable in the general form thus far. One of the methods used to estimate stability relies on the analysis of the effect of weak noise on chimera regimes [90, 95, 98]. The fact that chimera states are experimentally observed in a number of systems [99–105] favors the conjecture on their stability. In a general case, the question of a rigorous stability proof for chimera states remains open.

Among other, still not fully solved, problems, we mention the analysis of bifurcation mechanisms whereby one chimera structure or another, the statistical characteristics of these chimeras, their lifetimes, external and mutual synchronization, the role of external factors, and so on is realized. It is important to note that the existing research literature contains relatively few examples exploring chimera structures in ensembles composed of oscillators with chaotic dynamics, which present a rather broad class of auto-oscillatory systems. Besides, most publications deal with a single ensemble of identical oscillators. However, coupled ensembles, including those composed of different individual oscillators, are of special interest. In particular, one of the poorly studied questions in the dynamics of coupled ensembles is that of external and mutual synchronization between chimera structures [122–124]. The questions mentioned are not discussed in the two widely known reviews [65, 81], which present results of studies investigating ensembles of Kuramoto phase oscillators, FitzHugh–Nagumo and Stuart–Landau systems, Van der Pol oscillators, the effect of topology of coupling between oscillators, the role of delays in coupling networks, etc. But the dynamics of ensembles made of chaotic oscillators is not discussed. Systematic studies exploring the dynamics of ensembles of nonlocally coupled oscillators and mechanisms of spatio-temporal structure formation, including chimera states, in individual or interacting ensembles have been carried out at the Department of Radiophysics and Nonlinear Dynamics of Chernyshevsky Saratov National Research State University during the last five years. This review relies on the original research results published by the authors in collaboration with master's and PhD students of the department in leading national and international journals.

The review is organized as follows. After a brief introduction, we discuss the results of a pioneering study of the phase chimera in one-dimensional ensembles of logistic maps and Rössler oscillators with nonlocal coupling [55, 56]. We then proceed to the formation mechanism and characteristic properties of phase chimeras. We demonstrate that a chimera structure of a new type, called the amplitude chimera, can be realized. The mechanism behind its appearance, its statistical characteristics, and its lifetime are described. A hypothesis is further formulated and substantiated that chimera structures can form in ensembles of chaotic systems with a nonhyperbolic attractor, but typically they occur in ensembles of chaotic systems with a quasihyperbolic attractor. Based on this hypothesis, two basic models describing chimera structures in ensembles of nonlocally coupled chaotic systems are introduced. Next, spatio-temporal structures in two coupled ensembles are considered and a chimera structure of a new type — *the chimera of solitary states* — is described. General principles of chimera structure formation in ensembles of bistable oscillators are discussed. We conclude with an illustration of the effect of external and mutual synchronization of chimera structures in two symmetrically coupled ensembles of nonlocally connected logistic maps.

2. Phase chimera states in ensembles of nonlocally coupled logistic maps

Chimera structures in ensembles of chaotic nonlocally coupled oscillators were first explored in detail in Refs [55, 56]. The discrete logistic map [125, 126] and Rössler oscillator [127] in dynamic chaos regimes were taken as individual ensemble elements.

We consider the main results for a one-dimensional ensemble of nonlocally coupled logistic maps, described by the equation

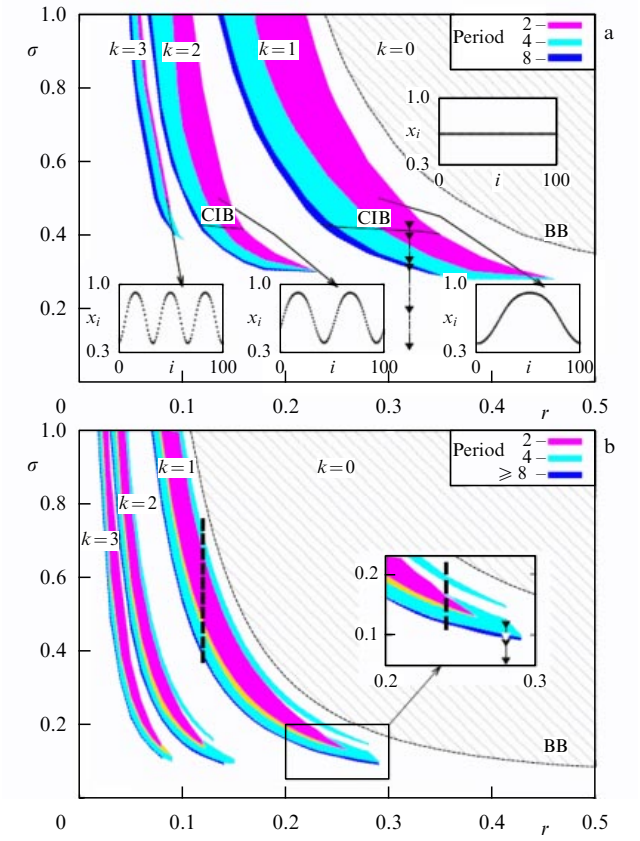

Figure 1. (a) Domains of coherence in the plane of parameters (r, σ) for $N = 100$ logistic maps (1) and (b) Rössler oscillators (3) labeled with the wave numbers k. The hatched domain ($k = 0$), corresponding to the regime of full chaotic synchronization, is delimited by the bifurcation line BB (blow-out bifurcation). Domains $k = 1, 2$, and 3 correspond to coherent regimes with the instantaneous oscillator amplitudes shown in the insets. Regimes of oscillations with period doubling are realized inside the 'tongues' of coherence. The lines CIB (coherence–incoherence bifurcation) separate regimes with coherent and incoherent dynamics. Parameters of systems: (a) $a = 3.8$, (b) $a = 0.42$, $b = 2.0$, $c = 4.0$. The arrows indicate the direction of change in the parameter σ for $r = 0.32$ for ensemble (1), which is described further below [56].

$$x_i^{t+1} = f(x_i^t) + \frac{\sigma}{2P} \sum_{j=i-P}^{i+P} \left(f(x_j^t) - f(x_i^t) \right), \qquad (1)$$

where x_i^t is a real-valued variable, t is the discrete time, $i = 1, 2, \ldots, N$ is the number of oscillators in the ensemble ($N = 100$), $f(x) = ax(1 - x)$ is the logistic map in a chaotic regime ($a = 3.8$), and σ is the nonlocal coupling coefficient between the oscillator i and P neighbors to the right and left. The coupling parameter σ and normalized coupling radius $r = P/N$ are used as the parameters governing system (1). Ensemble (1) is considered under periodic boundary conditions and typically for random initial conditions distributed in the interval $[0, 1]$. We note that system (1) describes the cases of local ($P = 1$), global ($P = N/2$), and nonlocal ($1 < P < N/2$) coupling. The coherence–incoherence transition is explored in the plane of parameters r and σ. The bifurcation diagram for system (1) is shown in Fig. 1a [56].

In [55], coherent states were understood as the regimes for which the instantaneous profiles of the amplitudes are sufficiently smooth and satisfy the condition

$$|x_{i+1}^t - x_i^t| < \delta, \quad \delta \ll 1, \quad t = \text{const}, \quad i = 1, 2, \ldots, N. \qquad (2)$$

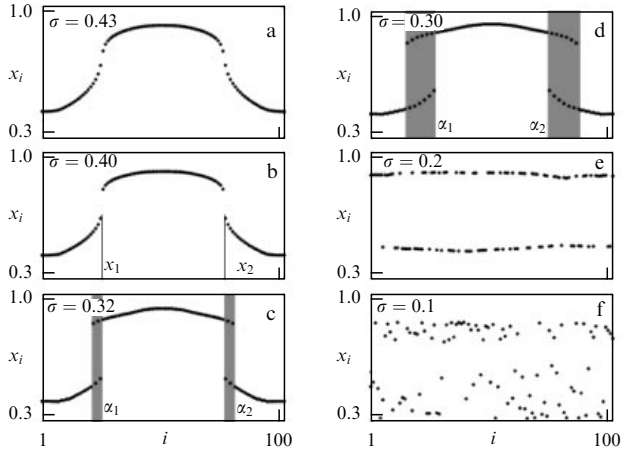

Figure 2. Evolution of instantaneous profiles of amplitudes in ensemble (1) for a decreasing σ for $r = 0.32$. The shaded regions α_1 and α_2 correspond to incoherent profiles [56].

Full synchronization of all ensemble elements corresponds to $\delta \to 0$ (for example, in the domain $k = 0$ in Fig. 1a).

For a decreasing coupling coefficient (in moving along the line shown in Fig. 1a), the authors of Refs [55, 56] describe the coherence–incoherence transition presented in Fig. 2. The smooth wavy profile x_i^t (Fig. 2a) breaks into the upper and lower branches (Fig. 2b). Then, as σ decreases, two regions with incoherent dynamics (α_1 and α_2) appear in the vicinity of points x_1 and x_2. The width of these regions increases as σ decreases (Fig. 2c, d). Further, the dynamics of ensemble elements become fully chaotic (incoherent) (Fig. 2e, f). In the α_1 and α_2 incoherence regions, the ensemble oscillators irregularly switch between the upper and lower branches of the instantaneous profile. As a result, a regime of coexisting coherent and incoherent clusters with sharp boundaries in the ensemble space is realized in ensemble (1). Put differently, a chimera state appears in ensemble (1), which fully corresponds to the definition given in Ref. [48].

Results of analytic computations of the critical value σ_{cr} of the coupling coefficient that corresponds to the appearance of a chimera state (the appearance of regions α_1 and α_2 in Fig. 2) were presented in [56]. As can be seen from Fig. 2, chimera state formation follows the formation of the vertical profile of instantaneous amplitudes with its subsequent breakup. Just this fact serves as a basis for the theoretical analysis of the mechanism whereby a chimera state is born in ensemble (1). It was concluded in [56] that for the map parameter $a = 3.8$, the critical value of the coupling parameter is $\sigma_{\text{cr}} \simeq 0.44$. Chimera states appear if $\sigma \leqslant \sigma_{\text{cr}}$.

A no less important result in Ref. [56] is a numerical analysis of the dynamics of a one-dimensional ring composed of Rössler oscillators with a nonlocal coupling introduced for all three phase variables:

$$\begin{aligned} \dot{x}_i &= -y_i - z_i + \frac{\sigma}{2P} \sum_{j=i-P}^{i+P} (x_j - x_i), \\ \dot{y}_i &= x_i + a y_i + \frac{\sigma}{2P} \sum_{j=i-P}^{i+P} (y_j - y_i), \\ \dot{z}_i &= b + z_i(x_i - c) + \frac{\sigma}{2P} \sum_{j=i-P}^{i+P} (z_j - z_i). \end{aligned} \qquad (3)$$

Figure 1b shows a bifurcation diagram obtained by analyzing the equations of ensemble (3) [56]. A comparison of the results shown in Fig. 1a and b indicates that dynamical regimes of ensembles of logistic maps (1) and Rössler oscillators (3) are topologically equivalent. This is an important point, and we return to it in what follows.

3. Formation mechanism and properties of phase chimeras

Analysis of the properties of chimera structures in rings composed of logistic maps and Rössler oscillators in Refs [55, 56] is undoubtedly important and fundamental. But these results do not answer a number of questions about the structure of the chimera found, its dynamical and statistical properties, or, finally, the question of whether chimeras of other types can be observed in systems (1) and (3). These questions are addressed in a set of papers published later [75, 91]. We digress to describe new results found there.

We turn once again to system (1), which can be rewritten as

$$x_i^{t+1} = ax_i^t(1 - x_i^t) + F(\sigma, r, x_i^t)\,, \tag{4}$$

where

$$F(\sigma, r, x_i^t) = \frac{\sigma}{2P} \sum_{j=i-P}^{i+P} \left(f(x_j^t) - f(x_i^t)\right), \tag{5}$$

and $f(x)$ is the logistic map. It follows from (4) that each ith ensemble oscillator experiences the action of P neighboring oscillators to the right and to the left. This net action $F(\sigma, r, x_i^t)$ is different for each ensemble oscillator with the number $i = 1, 2, \ldots, N$. The difference between the acting signals originating from nonlocal coupling leads to the formation of spatio-temporal structures of certain types in the ensemble. We refer to $F(\sigma, r, x_i^t)$ as the *coupling function*.

We consider ensemble (4) setting $a = 3.8$, $N = 1000$, and $P = 320$ ($r = P/N = 0.32$) and compute the coupling functions $F(x_i)$ for different values of σ. The left column in Fig. 3 shows the results of computing $F(x_i)$ in the form of spatio-temporal profiles that were constructed as follows. For each oscillator i, 20 to 50 values of the amplitude x_i^t were plotted, excluding the equilibration time, which comprised approximately 5×10^5 iterations of system (4) [91]. As a result of such a procedure, the dependences $F(x_i)$ give a qualitative idea of the temporal dynamics of each oscillator and its evolution in the ensemble space. Figure 3 clearly indicates that for $\sigma = 0.43$ (Fig. 3a), the function $F(x_i)$ describes periodic oscillations with period 2, and further, with a decrease in σ, it acquires period 4 (Fig. 3b), and for $\sigma = 0.3574$ (Fig. 3c), period 8.

Thus, with the reduction in the nonlocal coupling coefficient σ, the coupling function undergoes a cascade of period doubling bifurcations. The evolution of the front in the distribution of instantaneous amplitudes (the right column in Fig. 3) is seen in this case, with the front becoming vertical (Fig. 3b, c). And yet, this fact notwithstanding, the chimera structure is not observed. As $\sigma = 0.35$ is reached (Fig. 3d), the coupling function demonstrates the transition to a weakly chaotic regime characterized by two incoherence regions coexisting with coherence regions (Fig. 3d, right column). Thus, a chimera state is born. A further decrease in the coupling strength results in the widening of incoherence clusters, in the same manner as shown in Fig. 2.

We note that instantaneous profiles shown in Fig. 3 evolve with time because the ensemble oscillators continue to oscillate. Computations indicate that the time evolution of profiles does not modify the topology of the respective curves for the amplitude distribution in the ensemble space. For the coupling strength values that correspond to the data in Fig. 3a–c, the profiles remain smooth, satisfying the requirements in Eqn (2), which is the condition of coherence. For $\sigma = 0.35$ (Fig. 3d), the coherence breaks down for two small oscillator clusters, spawning a chimera state. Some information on the time evolution of instantaneous spatio-temporal amplitude profiles is also available in Fig. 5.

It can be concluded from the foregoing that the chimera state is related to the cascade of period doubling bifurcations in the coupling function $F(x_i)$ that occur as the nonlocal coupling coefficient σ decreases. The sequence of period doubling bifurcations terminates, leaving the regime of dynamic stochasticity, and the chimera state just follows this transition [48, 55, 75, 91].

We take a closer look at this type of chimera structure. Figure 4 depicts a numerically found instantaneous profile of amplitudes (Fig. 4a), time realizations $F(x_i^t)$ for two neighboring oscillators in an incoherent cluster of the chimera (Fig. 4b), and the crosscorrelation coefficient $\Psi_{1,i}$ (Fig. 4c).

It has been found in [75, 91] that in regions labeled as *1* and *2* in Fig. 4a, the oscillations are nearly periodic with the period 2, but differ by one time iteration (Fig. 4b). We say that in region *1*, all oscillators are 'in-phase', and in region *2*, they are 'anti-phase'. In regions of incoherence, the oscillators switch irregularly between the in-phase and anti-phase regimes (Fig. 4b). This effect breaks the coherence by creating regions of incoherence and hence the chimera state.

We analyze the cause and mechanism of switching the 'phase' of oscillators. With this aim, we return to Fig. 3 (right column) and construct spatio-temporal profiles for these regimes (Fig. 5). Numerical data in Fig. 5a correspond to an instantaneous profile of the amplitudes in Fig. 3a (right column). From the plot, it can be seen that the oscillators with numbers $i = 298$ and $i = 798$ are in a fixed-point regime, whereas all other oscillators perform oscillations with the period 2. For the specified oscillators, the coupling function $F(x_i)$ vanishes, as can be seen from Fig. 3a (left column). Equation (4) then allows determining a fixed point of period 1

$$x^0 = 3.8x^0(1 - x^0)\,, \quad x^0 = 0.737\,. \tag{6}$$

This value corresponds to the result presented in Fig. 5a. It can be easily verified that the equilibrium state x^0 is unstable. As follows from a detailed analysis [75, 91], all the oscillators with numbers $i < 298$ perform in-phase oscillations, whereas those with numbers $298 < i < 798$ are in anti-phase. The change in the phase of oscillations (one iteration shift) occurs in space on passing along the ensemble through the oscillator $i = 298$. As can be seen from Fig. 5a, on approaching the oscillator $i = 298$, the amplitude of oscillations decreases, becoming zero at $i = 298$, and then starts to increase for $i > 298$. This is accompanied by an abrupt change in the 'phase' of oscillations. Because the initial conditions for system (4) are taken as randomly distributed in the interval $[0, 1]$ and the equilibrium state $x^0 = 0.737$ is unstable, oscillators with in-phase and anti-phase dynamics alternate irregularly close to $i = 298$. One incoherence cluster of the chimera state is thus formed.

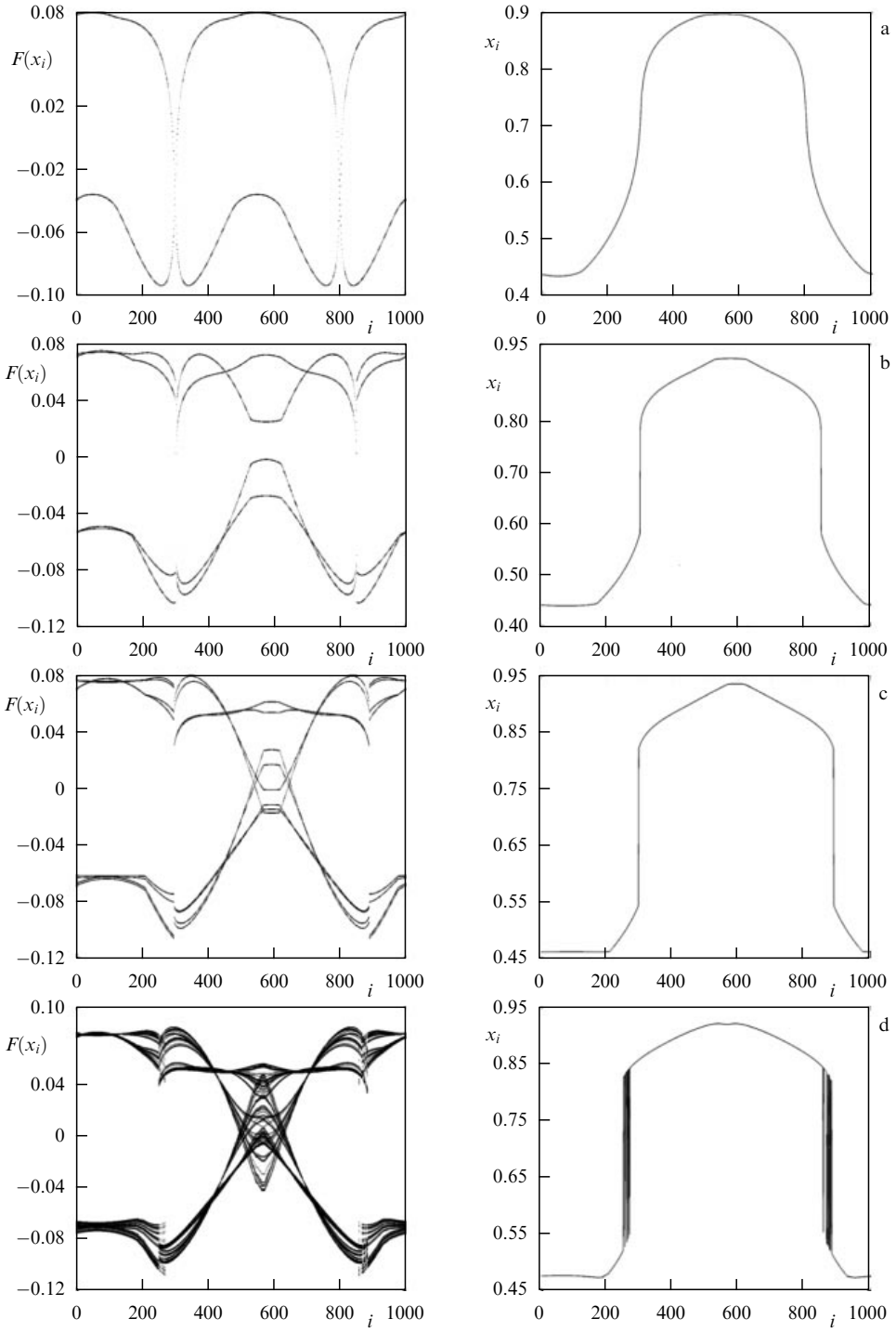

Figure 3. Spatio-temporal profiles of the coupling function F_i (left) and instantaneous profiles of the amplitudes x_i ($t = \text{const}$) (right) for the coupling coefficient σ: (a) 0.43, (b) 0.38, (c) 0.3574, and (d) 0.35. The other parameters are $a = 3.8$, $r = 0.32$, and $N = 1000$.

The alternation of in-phase and anti-phase oscillations in the incoherent cluster of a chimera structure can be illustrated quantitatively by using the crosscorrelation coefficient (CC) for different ensemble elements [77, 86]. We consider the first ($i = 1$) and ith oscillators at the same given moment of time. Then the CC is defined as

$$\Psi_{1,i} = \frac{\langle \tilde{x}_1(t)\tilde{x}_i(t)\rangle}{\sqrt{\langle \tilde{x}_1^2(t)\rangle\langle \tilde{x}_i^2(t)\rangle}}\,, \quad \tilde{x}(t) = x(t) - \langle x(t)\rangle\,, \qquad (7)$$

where the angular brackets denote time averaging.

Figure 4c displays the results of CC computations using formula (7) for the chimera state regime shown in Fig. 4a. As can be seen from this figure, in the incoherent clusters of the chimera, the CC values alternate, being either $\simeq +1$ or $\simeq -1$. A decay of correlations is not observed, only a change of sign. This quantitatively confirms the fact that the oscillations in regions *1* and *2* are practically periodic with the period 2 and differ only by a half-period phase lag (one iteration with time). We mention that $|\Psi_{1,i}| \simeq 0.95 < 1$. This happens because the oscillations correspond to a weak chaos regime and fail to be strictly periodic, as mentioned already.

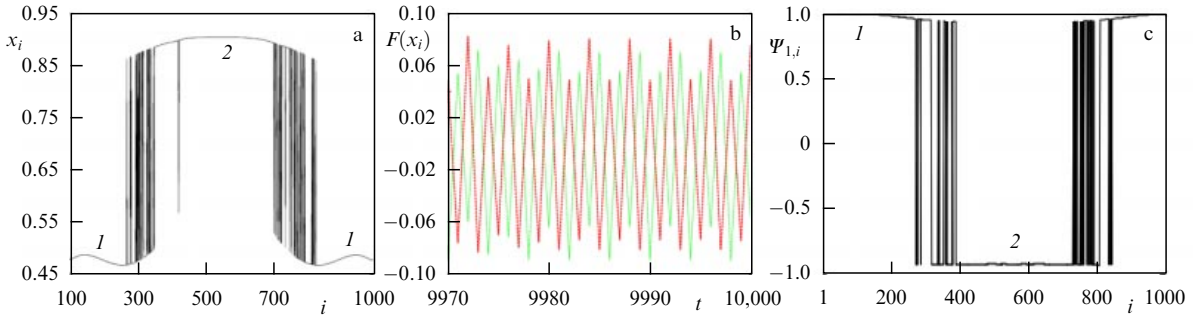

Figure 4. (a) Instantaneous profile x_i ($t = \text{const}$) computed for $\sigma = 0.27$ using Eqns (4); (b) temporal realizations of the function $F(x_i(t))$ for two neighboring elements $i = 318$ and $i = 319$ from the incoherence region, and (c) the crosscorrelation coefficient $\Psi_{1,i}$ in Eqn (7) for the chimera structure shown in panel a. All other parameters are as in Fig. 3.

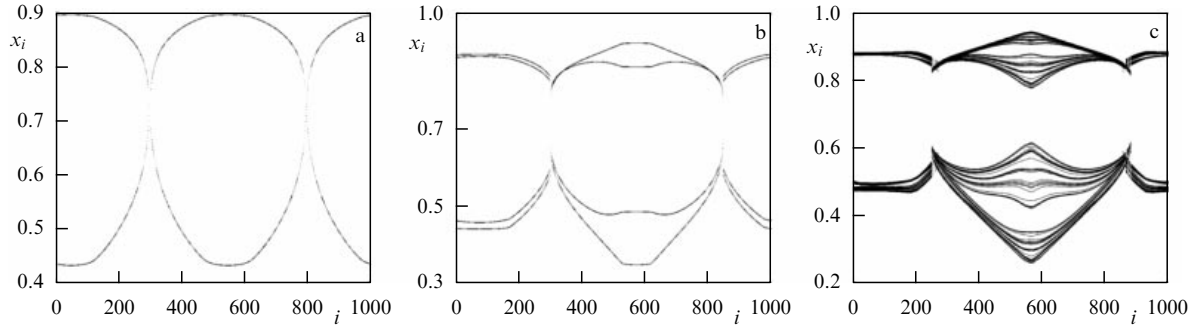

Figure 5. Spatio-temporal profiles of the amplitudes x_i for three values of the coupling strength σ: (a) 0.43, (b) 0.38, and (c) 0.35. The other parameters are the same as in Fig. 3.

The properties of such a chimera state, described in detail above, gave us grounds to call it the *phase chimera* [75, 91]. As shown in Section 4, this chimera type is not the only one. Ensemble (1) allows another type of spatio-temporal structure, which we called the *amplitude chimera* [75, 91].

4. Amplitude chimera states

Studies of coherence–incoherence transitions in ensemble (4) showed that a decrease in the nonlocal coupling parameter σ to values smaller than the critical value $\sigma_{\text{cr}} \simeq 0.44$ leads to the appearance of incoherence regions (see Figs 3 and 4). A chimera state called the phase chimera is born. But what happens in ensemble (4) if σ is decreased further, keeping $r = 0.32$ fixed? The research shows that in this case a new cluster of incoherent dynamics can be created for a finite number of ensemble oscillators, shown in Fig. 6. Figure 6a illustrates a cluster of oscillators $120 \leqslant i \leqslant 280$ with various instantaneous oscillation amplitudes. From the plot of the coupling function $F(x_i)$ (Fig. 6b), it is clearly seen that oscillators in the indicated range of i are under the action of a chaotic signal. As a result of this action, the oscillators of an incoherent cluster demonstrate chaotic dynamics [75, 91].

Computations showed that the incoherent cluster $120 \leqslant i \leqslant 280$ is characterized by an irregular distribution of the oscillation amplitudes x_i, whereas the oscillators in the ensemble outside the incoherent cluster perform oscillations with a period close to 4. Studying the dynamics of individual oscillators in the incoherent cluster (the analysis of temporal realizations of the $x_i(t)$) indicated that oscillations exhibit a pronounced chaotic character and are characterized by an exponential instability. The specific features of the cluster, reflecting irregularity in the amplitudes of cluster oscillators,

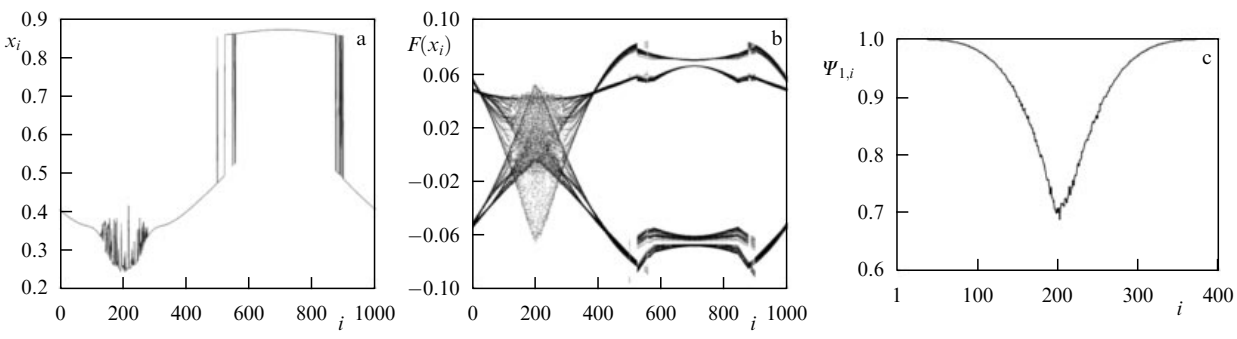

Figure 6. Illustration of the amplitude chimera in ensemble (4) for $\sigma = 0.28$. (a) The profile of instantaneous amplitudes, (b) the spatio-temporal profile of the coupling function $F(x_i)$, and (c) the dependence of the CC $\Psi_{1,i}$ for oscillators of the amplitude chimera cluster. The other parameters are the same as in Fig. 3.

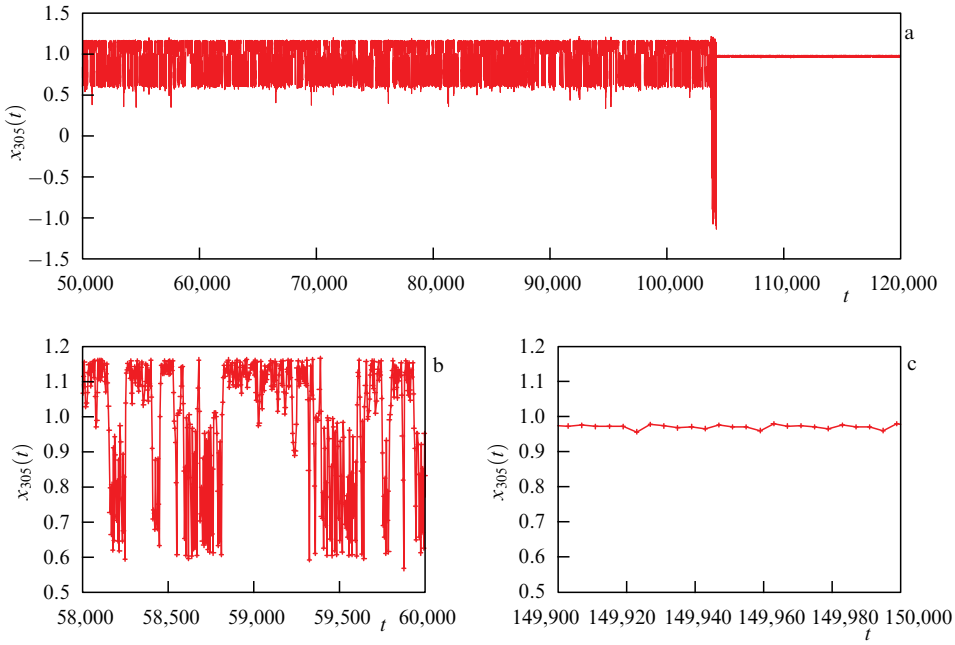

Figure 7. Temporal realization of $x(t)$ for the amplitude chimera oscillator $i = 305$ in ensemble (8) illustrating (a) switching the amplitude chimera over into the regime of phase chimera after a finite number of iterations $t \simeq 105{,}000$, (b) the regime of irregular transitions with time for the same chimera element, and (c) the amplitude $x(t)$ after switching over to the regime of phase chimera, sampled after a period of oscillations. The parameters of system (8): $\sigma = 0.304$, $r = 0.32$, $N = 1000$, $\alpha = 1.4$, and $\beta = 0.3$.

motivated calling the chimera state of the described type the *amplitude chimera* [75, 91].

To quantitatively describe the incoherence of oscillations in the amplitude chimera regime (Fig. 6a), CC (7) has been computed [77, 86]. The amplitudes of chaotic oscillations in the incoherent cluster are confined to two chaotic subsets. As follows from computations, the phase trajectories of individual elements in the amplitude chimera cluster regularly switch over between these subsets with the period 2. To eliminate the periodic component from the realization of $x_i(t)$, we sampled amplitudes every second iteration, i.e., we considered values of $x_i(t)$ at discrete moments of time $t = 1, 3, 5, \ldots$. The computed CC $\Psi_{1,i}$ are plotted in Fig. 6c.

As follows from Fig. 6c, the CC $\Psi_{1,i}$ is close to unity for oscillators in the coherent state to the right and to the left of the incoherent cluster of the amplitude chimera, and it sharply drops to $\simeq 0.7$ in the incoherence cluster $120 < i < 280$. Computations confirm the fact that the oscillators in the amplitude chimera cluster are uncorrelated and hence incoherent [77, 86].

Numerical studies revealed general properties of phase and amplitude chimera states in ensembles of chaotic oscillators where chaos is realized as a result of period doubling bifurcations. The studies involved ensembles of nonlocally coupled double-dimensional Hénon maps [66, 87, 88], cubic [93], and sinusoidal maps, as well as time-continuous systems: Rössler and Anishchenko–Astakhov oscillators [91, 128, 129] and the Chua chain [93, 130]. Details and differences among the regimes of phase and amplitude chimera were uncovered.

In all these ensembles, phase chimeras are characterized by periodic oscillations in incoherent clusters with an irregular phase shift between oscillators. The lifetime of phase chimeras in numerical experiments is practically unlimited. The phase chimeras persist in ensembles of discrete maps for more than 10^8 iterations.

The properties of amplitude chimera regimes are different. Detailed studies of time realizations of the $x_i(t)$ for oscillators from a cluster of amplitude chimeras demonstrated the following. First, temporal oscillations are nonstationary and represent a process of irregular intermittency between several distinct regimes. Most often, the intermittency occurs between the regimes of phase and amplitude chimeras. Second, amplitude chimeras have a finite lifetime.

As an example, Fig. 7 displays computation results for an ensemble of nonlocally coupled Hénon maps [90]. The ensemble equations are analogous to (1), but individual elements are described by a double-dimensional map:

$$x_i^{t+1} = f(x_i^t, y_i^t) + \frac{\sigma}{2P}\sum_{j=i-P}^{i+P}\left(f(x_j^t, y_j^t) - f(x_i^t, y_i^t)\right),$$

$$y_i^{t+1} = \beta x_i^t, \quad f(x_i^t, y_i^t) = 1 - \alpha(x_i^t)^2 + y_i^t. \tag{8}$$

The finite lifetime and nonstationarity of oscillations of the oscillators from an incoherent cluster of an amplitude chimera suggest that chimera states of this type can be classified as *transient chimera states* [78].

5. Role of quasihyperbolicity of chaotic attractors

It has been found from numerical experiments that the spatio-temporal structures in ensembles of nonlocally coupled oscillators with period doubling are not encountered in ensembles of Lorenz systems. A system of nonlocally coupled Lorentz oscillators

$$\dot{x}_i = -\gamma(x_i - y_i) + \frac{\sigma}{2P}\sum_{j=i-P}^{i+P}(x_j - x_i),$$

$$\dot{y}_i = -x_i z_i + \rho x_i - y_i + \frac{\sigma}{2P}\sum_{j=i-P}^{i+P}(y_j - y_i), \tag{9}$$

$$\dot{z}_i = -bz_i + x_i y_i$$

was explored in [131] for values of parameters that correspond to the classical Lorenz attractor [132–135]: $\rho = 28$, $\gamma = 10$, and $b = 8/3$. The number of oscillators in the ensemble is $N = 100$. An analysis of the dynamics of ensemble (9) on the (r, σ) parameter plane, where $r = P/N$, indicated that the coherence–incoherence transition occurs in this system through the regimes of so-called *solitary states* and traveling waves [131]. No chimera states were found in this case! A basic question is why? The answer is given in Ref. [66].

The absence of chimera structures in ensemble (9) comes from a fundamental difference between the chaotic attractor in the individual Lorenz system and the chaotic attractors forming via a cascade of period doubling bifurcations according to the Feigenbaum scenario [136]. The Lorenz attractor is quasihyperbolic and in numerical experiments can be considered hyperbolic because it does not include stable regular subsets such as fixed points or limit cycles [134, 135, 137]. For Lorenz-type attractors, multistability is excluded, and a chaotic attractor is the only attracting set in the system phase space.

The authors of [66] formulated a hypothesis that chimera states in ensembles of nonlocally coupled chaotic oscillators occur only when chaotic attractors of individual oscillators are nonhyperbolic [138, 139] and are characterized by multistability. If the chaotic attractors are in the quasihyperbolic (or hyperbolic) class, chimera states are not realized in the ensembles. As a characteristic example, an ensemble of nonlocally coupled Lorenz oscillators (9) was considered in [66] for parameter values $\rho = 220$, $\gamma = 10$, and $b = 8/3$, when the attractor in the Lorentz system loses its property of quasihyperbolicity, becoming nonhyperbolic. Chimera states were obtained in this case.

Based on the results in Ref. [66], it was proposed to introduce two basic models to describe the mechanisms and properties of chimera structures in ensembles of chaotic systems: Hénon [140] and Lozi [141] maps.

Double-dimensional Hénon map (8) is typical for the description of chaotic systems with a so-called spiral Shilnikov attractor [142]. As $\beta \to 0$, system (8) transforms into the logistic map. Furthermore, for spiral attractors in three-dimensional differential systems of the Rössler type, a double-dimensional map is realized in the Poincaré section, which is topologically equivalent to the Hénon map [143, 144].

As the second basic model, using the Lozi map [141]

$$x_{n+1} = 1 - \alpha|x_n| + y_n\,, \quad y_n = \beta x_n \tag{10}$$

was proposed in [66]. As is known, the Lozi map was introduced especially to describe the subcritical excitation mechanism and properties of the classical Lorenz attractor [132, 134, 135, 145]. Map (10) is quasihyperbolic: as $\beta \to 0$, it transforms into a classical hyperbolic 'tent map'. In the Poincaré section by a double-dimensional plane, the Lozi map serves as a model to describe a wide class of three-dimensional differential systems with a Lorenz-type attractor.

Thus, using the basic Hénon (8) and Lozi (10) maps as elements of ensembles with nonlocal coupling results in a sufficiently general model of ensembles of chaotic oscillators with both discrete and continuous time.

In a one-dimensional ensemble of nonlocally coupled Hénon maps, as shown in Refs [66, 87, 88], all types of spatio-temporal structures resembling those described above are realized. Furthermore, for $\beta = 0.3$ (for sufficiently strong contraction in phase space), the bifurcation diagram of regimes in the plane of coupling parameters for a ring of Hénon maps practically repeats the diagram for a ring of logistic maps (Fig. 1a). Not only qualitative but also quantitative correspondence takes place [66, 87, 88]. For this reason, we do not discuss the details of the coherence–incoherence transition in ensembles of nonlocally connected Hénon maps. In the ensemble of Lozi maps, as expected, the transition from full chaotic synchronization to spatio-temporal chaos (complete incoherence) occurs differently [66, 87, 88].

6. Coherence–incoherence transition in an ensemble of Lozi maps

We consider the dynamics of ensemble (8) using Lozi map (10) as its individual oscillator. It was shown in [87, 88] that the transition from the regime of full chaotic synchronization to that of spatio-temporal chaos also occurs in this ensemble when the strength of nonlocal coupling σ is varied. However, first, this transition occurs through the regime of so-called solitary states [131] and, second, the regimes of chimera states are not observed in this case. We consider the bifurcation diagram for the Lozi ring regimes shown in Fig. 8.

This bifurcation diagram qualitatively resembles the one for the ring of logistic maps (see Fig. 1) by the presence of the coherence regions A, C, and D and spatio-temporal chaos B. However, the transition from the region of chaotic synchronization A to region B proceeds through the regime of solitary states, and in the regions painted white, the regimes of traveling waves are observed, as in the ensemble of coupled Lorenz oscillators [131].

We consider the regime of solitary states in some detail. If the transition from region A to region B is made by varying the coupling parameter, then the picture presented in Fig. 9 is realized. For $\sigma = 0.226$, a sharp amplitude spike for one oscillator appears in the instantaneous profile (Fig. 9a). A further reduction in the coupling parameter leads to an increase in the number of oscillators in the regime of amplitude spikes (Fig. 9b, c), finally leading to the regime of spatio-temporal chaos. We stress that chimera states were not found in this transition. The mechanism spawning solitary states operates through a change in the properties of individual ensemble oscillators under the action of nonlo-

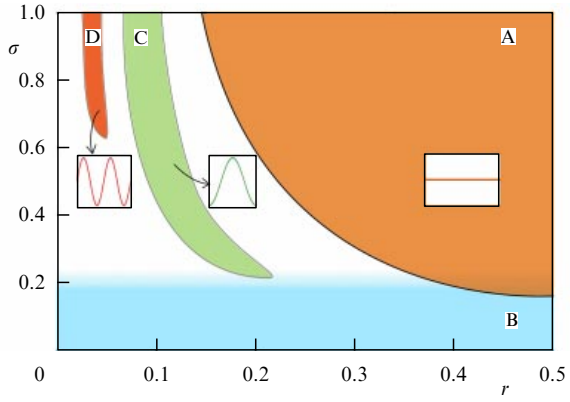

Figure 8. Bifurcation diagram in the plane of parameters (r, σ) for an ensemble of nonlocal coupled Lozi maps (10). Regions A and B respectively correspond to full chaotic synchronization and the spatial incoherence regime. The coherent spatial profiles (shown in the insets) are realized in region C with the wavenumber $k = 1$ and in region D with $k = 2$. The ensemble parameters are $\alpha = 1.4$ and $\beta = 0.3$.

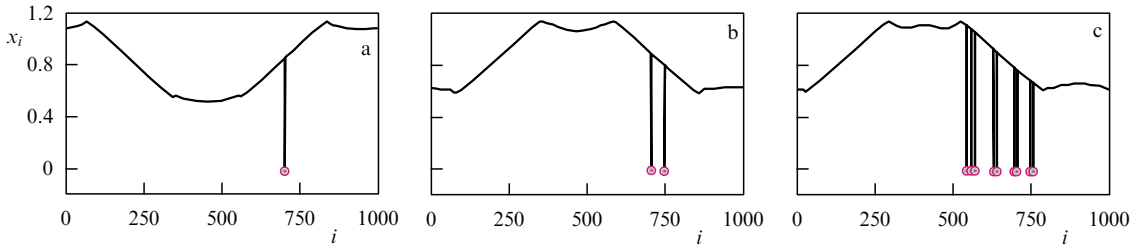

Figure 9. Regimes of solitary states in a ring of coupled Lozi maps (10) for $r = 0.2$ for a decreasing coupling parameter σ: (a) 0.226, (b) 0.225, and (c) 0.223. An amplitude spike appears in (a), there are two of them in (b), and even more appear in (c).

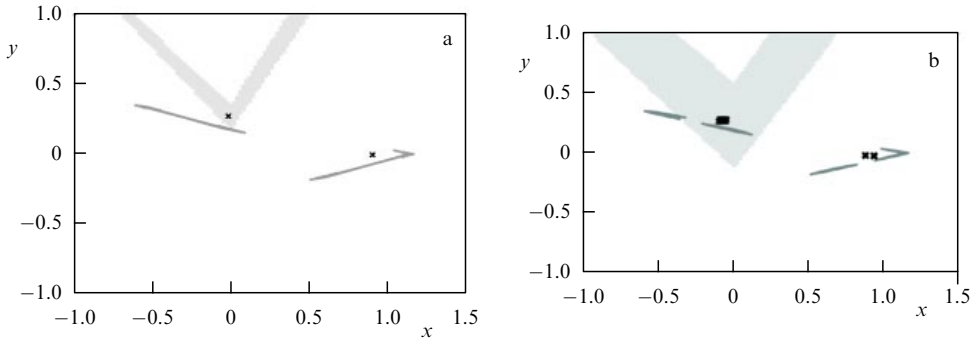

Figure 10. Attractors of system (11) for the coupling parameter σ (a) 0.226 and (b) 0.2. Gray shading marks attraction basins of solitary state attractors computed for a selected ensemble oscillator.

cally coupled neighboring oscillators. Our studies showed that the dynamics of an individual Lozi oscillator in the ensemble become substantially modified under the action of P neighboring oscillators from the right and left. The Lozi system loses its hyperbolic character under the external action and becomes bistable. The spikes in amplitudes in Fig. 9 just correspond to the 'switch over' of phase trajectories to the second attractor because of random initial conditions. As the coupling coefficient σ decreases, the attraction basin of the second attractor widens. The number of solitary states also increases, which is reflected in Fig. 9.

We pause here to clarify the details. By simple manipulations, ring equations (8) can be rewritten in the form

$$\begin{aligned} x_i^{t+1} &= (1-\sigma) f(x_i^t, y_i^t) + \frac{\sigma}{2P} \sum_{j=i-P}^{i+P} f(x_j^t, y_j^t)\,, \\ y_i^{t+1} &= \beta x_i^t\,. \end{aligned} \tag{11}$$

It follows from system (11) that under the influence of nonlocal coupling, the coupling coefficient modifies the form of each individual oscillator: the factor $(1-\sigma)$ appears in the first term in the right-hand side of (11), and this oscillator works in a nonautonomous regime, affected by P neighboring oscillators (second term) via nonlocal coupling. Owing to these modifications, individual oscillators in the ensemble acquire fundamentally new properties. A special study of a ring of Lozi maps showed that individual ensemble oscillators acquire the bistability property by virtue of (11): a new attractor emerges close to the Lozi attractor in phase space. The attraction basin of the new attractor is rather narrow and widens with the decrease in the coupling coefficient. The results of computations are shown in Fig. 10.

Because of random initial conditions, one ensemble oscillator turns out to be in a narrow attraction basin (Fig. 10a) passing to the solitary state regime. As the coupling coefficient is decreased, the attraction basins widen (Fig. 10b), and increasingly more oscillators are in the regime of solitary states. Their number increases linearly with the decrease in the coupling coefficient. In the limit $\sigma \to 0$, the ensemble contains N uncoupled Lozi oscillators in the chaotic regime and a transition to the regime of spatio-temporal chaos occurs.

7. Chimera of solitary states in coupled ensembles of Hénon and Lozi maps

We consider a system of two interconnected ensembles with a nonlocal coupling, consisting of one-dimensional rings of Hénon and Lozi oscillators

$$\begin{cases} x_i^{t+1} = f(x_i^t, y_i^t) + \dfrac{\sigma_1}{2P} \displaystyle\sum_{j=i-P}^{i+P} \left[f(x_j^t, y_j^t) - f(x_i^t, y_i^t) \right] + \gamma F_i^t\,, \\ y_i^{t+1} = \beta x_i^t\,; \end{cases}$$

$$\begin{cases} u_i^{t+1} = g(u_i^t, v_i^t) + \dfrac{\sigma_2}{2R} \displaystyle\sum_{j=i-R}^{i+R} \left[g(u_j^t, v_j^t) - g(u_i^t, v_i^t) \right] - \gamma F_i^t\,, \\ v_i^{t+1} = \beta u_i^t\,, \quad i = 1, 2, \ldots, N\,, \ N = 1000\,. \end{cases} \tag{12}$$

The first system of equations in (12) describes a ring of nonlocally coupled Hénon maps ($f(x,y) = 1 - \alpha x^2 + y$). The parameter of nonlocal coupling σ_1 and the number of nearest neighbors P of the ith element to the right and to the left are selected such that a chimera state is observed in an isolated ensemble of Hénon maps. The second system of equations in (12) describes a ring of nonlocally connected Lozi maps ($g(u,v) = 1 - \alpha|u| + v$). The coupling parameters σ_2 and R are chosen such that the ensemble of Lozi maps demonstrates the regime of solitary states in the absence of coupling to the ring of Hénon maps. The governing parameters of individual elements in (12) are selected as $\alpha = 1.4$, and $\beta = 0.3$, which

corresponds to chaotic behavior in all individual elements of the system considered in the absence of coupling. The two rings are coupled symmetrically via the coupling function F, which in the case of dissipative or inertial coupling between the rings takes the respective form

$$F_i^t = g(u_i^t, v_i^t) - f(x_i^t, y_i^t) \quad \text{or} \quad F_i^t = u_i^t - x_i^t \,. \tag{13}$$

The coefficient γ characterizes the strength of symmetric coupling between the ith oscillators in the Hénon and Lozi rings.

As a result of numerical studies, it has been found [124] that with a variation in parameters in system (12), spatio-temporal structures can be realized that can be found in individual (uncoupled) Hénon and Lozi ensembles. For example, when the parameter of symmetric coupling γ is varied, the regimes of phase and amplitude chimeras can be realized in the Lozi ring, and the regimes of solitary states and traveling waves can be realized in the Hénon ring. In addition to the structures mentioned, for both dissipative and inertial coupling types in system (12), a new type of chimera state can be realized that we call the chimera of solitary states, a chimera structure including solitary states [124]. The new structure is realized in the ensemble of Hénon oscillators for a small value of the coupling parameter γ; its form is presented in Fig. 11.

An incoherent cluster of a solitary state chimera includes a group of oscillators ($300 < i < 500$ in Fig. 11) in the regime of solitary states, which, unlike the phase chimera, are in a weakly chaotic regime. The new structure is insensitive to small variations in the initial conditions, and it is realized in a finite domain of the governing parameters of system (12). Studies of the properties of the amplitude chimera in the system of coupled ensembles (12) demonstrated full correspondence of its properties to those described above for an individual ring of logistic maps. The amplitude chimera also exhibits nonstationarity of oscillations for all cluster oscillators and typically a finite lifetime. However, in a system of two coupled rings, the lifetime of amplitude chimeras can be controlled in wide limits by varying the coupling coefficient γ. The dependence of the lifetime on the parameter γ is essentially nonlinear in this case.

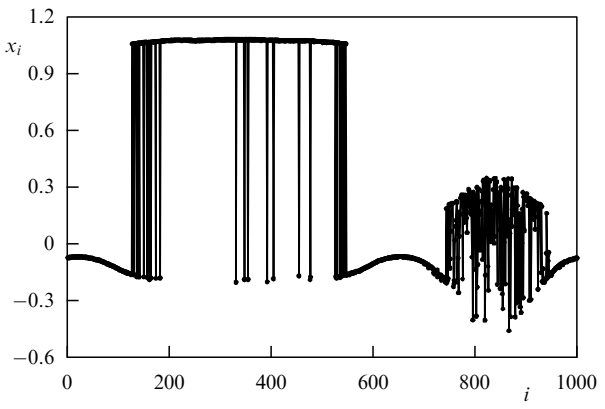

Figure 11. Instantaneous profile of the dynamics of an ensemble of Hénon maps in coupled system (12) illustrating the coexistence of solitary state and amplitude chimeras for a weak coupling $\gamma = 0.005$. The system parameters are $\alpha = 1.4$, $\beta = 0.3$, $\sigma_1 = 0.32$, $\sigma_2 = 0.225$, $P = 320$, and $R = 190$.

Special studies have demonstrated that the mechanism of solitary state chimera formation qualitatively corresponds to that described in Section 6 (see Fig. 10). Owing to nonlocal coupling, two close attractors emerge in the phase space of system (12) that correspond to the coherent regime and the regime of solitary states, and the system becomes bistable.

8. Realization mechanisms of solitary state regimes and the solitary state chimera in a one-dimensional ensemble of nonlocally coupled Hénon maps

In Section 6, we discussed the mechanism leading to solitary states in an ensemble of Lozi maps. The ensemble equations are given by (8), where $f(x_i^t, y_i^t)$ should be taken as Lozi map (10). It was shown that the reason behind the occurrence of the solitary state regime is the loss of quasihyperbolicity by the Lozi map and the appearance of bistability (see Fig. 10). It is natural to suppose that similar dynamics can be demonstrated by a one-dimensional ring of oscillators of Hénon maps, because an individual Hénon map is by definition a nonhyperbolic system. The results in Ref. [146] confirmed this fact. It was found that solitary state regimes and chimeras of solitary states are indeed realized in a one-dimensional ring of Hénon oscillators (8) and are caused, as for a Lozi ring, by the bistability effect. We consider these results in more detail.

To demonstrate the presence of bistability, we add a noise perturbation to the coupling coefficient in system (8) by taking

$$\sigma = \sigma_0(1 + \sqrt{2D}\xi^t) \,, \tag{14}$$

where D is the intensity of noise distributed uniformly from -1 to 1, and ξ^t is the noise source. If the system is bistable, then, under the action of noise, its phase trajectories could intersect the separatrix surface between the attraction basins of its attractors. Computations confirmed this fact. Under the action of noise, regimes of solitary states are indeed realized in the Hénon ensemble [146]. Phase portraits of the emerging attractors and their attraction basins in the plane of variables (x_i, y_i) were constructed based on numerical simulations for an oscillator in the solitary state regime. Figure 12a plots computed attractors for the oscillator $i = 721$ under various initial conditions (x_i^0, y_i^0). As can be seen from Fig. 12a, the phase portrait reflects the presence of two attractors, shown in black (attractor 1a, b) and gray (attractor 2a, b). The first corresponds to the solitary state of oscillator $i = 721$. The second attractor corresponds to the dynamics of an oscillator in the coherent domain.

Each attractor contains two attracting subsets (labeled a and b), and the phase trajectory switches regularly between them at every time iteration.

Figure 12b shows the computed attraction basins for attractors 1a and 2a. Under the action of noise, phase trajectories intersect the separatrix and find themselves in the attraction basin of attractor 1 related to the solitary state. The effects of switching between bands a and b is illustrated in Fig. 12c. It is seen that oscillations at attractors 1 and 2 are aperiodic, with a phase lag of one iteration, and contain a regular component of period 2.

The results shown in Fig. 12 are obtained under the action of weak noise $D = 0.000815$, which triggered switching the system over from attractor 2 to attractor 1. It was found that the

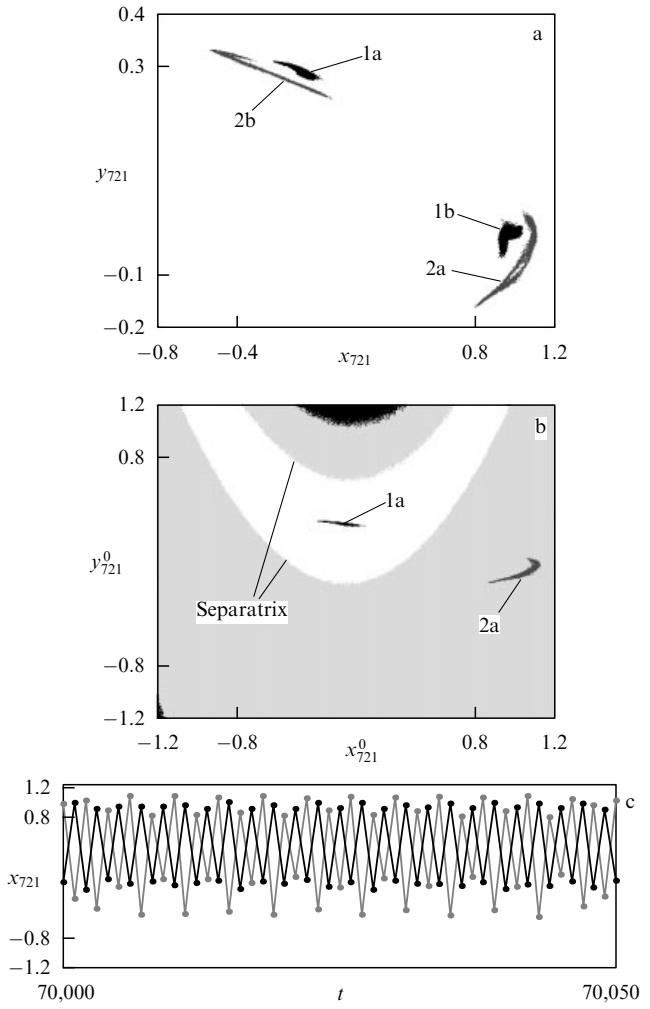

Figure 12. (a) Attractors for oscillator $i = 721$: 1a, b correspond to the solitary state regime, 2a, b correspond to the coherent domain. (b) The attraction basins for attractors 1a (white) and 2a (gray); the black region corresponds to trajectories escaping to infinity. (c) Temporal realizations x^t_{721} on the attractor 1a, b (gray dots) and 2a, b (black dots). Even iterations correspond to bands a, and odd to bands b. The parameters of system (8) are $\sigma_0 = 0.282$, $r = 0.32$, and $D = 0.000815$.

switching is also realized in the absence of noise [146]. This depends on two factors: the character of the random distribution of initial conditions and the form of the ensemble spatio-temporal structure, i.e., on the selected parameters P and σ in system (8). If the regime with coexisting phase and amplitude chimeras of the type shown in Fig. 6a is initially realized in model (8), then, under random initial conditions, the regime of a solitary state chimera can emerge in system (8) (Fig. 13a). If an amplitude chimera exists in the system, the attraction basins of attractors 1 and 2 change their structure, manifesting a riddling effect [147–149]. Riddling of the attraction basin of attractor 1 (the white region in Fig. 13b) raises the probability that the system would switch ower to the regime of solitary states and leads to the appearance of the solitary state chimera structure. Thus, the results presented in Figs 12 and 13 indicate that the regimes of solitary states and the chimera of solitary states are realizable in a one-dimensional ring of nonlocally coupled Hénon maps.

9. Double-well chimeras in ensembles of bistable oscillators with a nonlocal coupling

Among dynamical systems with regular and chaotic dynamics, a wide class of so-called bistable systems can be singled out. The bistable dynamics are demonstrated by physical [150, 151], radio-electronic [130], chemical [152], biological [153, 154], and other systems [155, 158]. Spatio-temporal structures in ensembles of coupled oscillators such as discrete cubical maps, FitzHugh–Nagumo oscillators, and the Chua chain in regimes of bistable dynamics were explored in [93, 95]. A new type of chimera structure was discovered, called the *double-well chimera* in Ref. [95]. As an example, we consider a double-dimensional ensemble of nonlocally coupled cubic maps described by the system of equations [95]

$$x^{t+1}_{i,j} = f(x^t_{i,j}) + \frac{\sigma}{B} \sum_{k=i-R,\,p=j-R}^{i+R,\,j+R} \Big[f(x^t_{k,p}) - f(x^t_{i,j}) \Big],$$
$$i, j = 1, \ldots, N, \qquad (15)$$
$$f(x) = (\alpha x - x^3) \exp\left[-\frac{x^2}{\beta} \right], \quad B = (1 + 2R)^2 - 1,$$
$$x^t_{i+N,j} = x^t_{i,j}, \quad x^t_{i,j+N} = x^t_{i,j}.$$

The indices i and j specify the element position in the lattice and are treated as spatial coordinates (x and y, respectively), and $t = 0, 1, 2, \ldots$ is the discrete time. The function $f(x)$ determines the dynamics of an individual map and depends on the parameters α and β. The size of the system is N, the number of elements in one direction (along the x or y axis). Boundary conditions are periodic in both directions. The

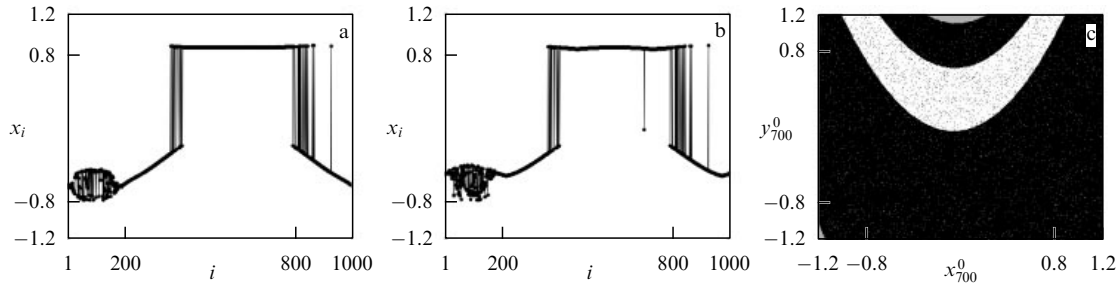

Figure 13. (a, b) Instantaneous profiles in the regime with coexisting amplitude and phase chimeras for various initial conditions for oscillator $i = 700$: (a) in the attraction basin of the attractor from the coherent domain (black domain in panel c) and (b) in the attraction basin of the attractor of solitary states (white region in panel c); (c) attraction basins of subsets 1a (white domain) and 2a (black domain) (see Fig. 12) for oscillator $i = 700$. Small grains in the attraction basins of attractors 1 and 2 characterize the riddling effect. The parameters of system (8) are $\sigma_0 = 0.282$, $r = 0.32$, and $D = 0$.

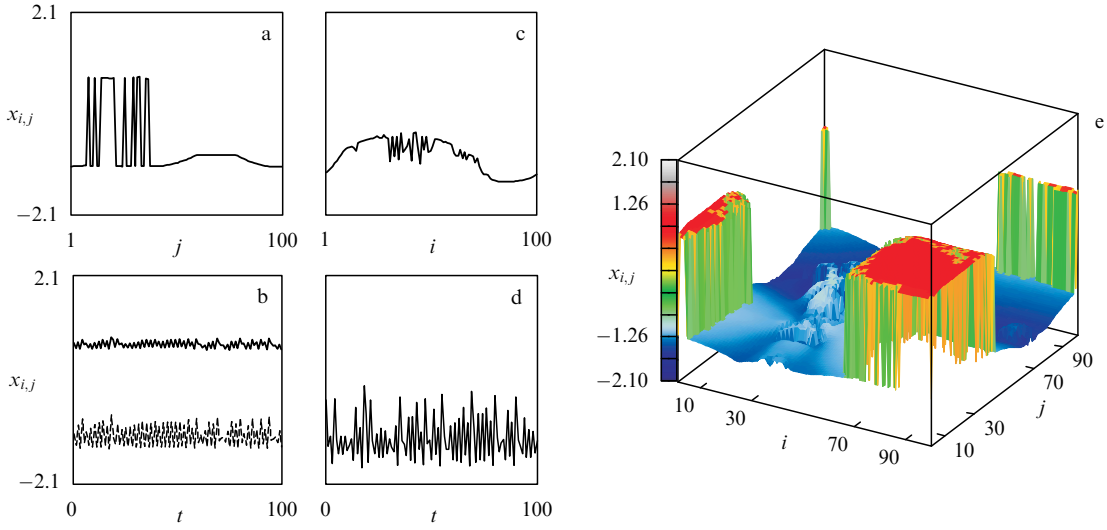

Figure 14. A double-well chimera in system (15) for $r = 0.35$, $\sigma = 0.444$. (a–d) Spatial sections and temporal realizations of oscillations for selected elements. Shown are (a) the spatial section $j = 6$ and (b) the temporal realization of oscillations for two neighboring elements $i = 49$, $j = 6$ and $i = 50$, $j = 6$ corresponding to the lattice part with a double-well chimera; (c) the spatial section $j = 50$ and (d) a temporal realization of oscillations for element $i = 31$, $j = 50$ corresponding to the lattice part with an amplitude chimera. Panel (e) shows a three-dimensional snapshot of an instantaneous lattice state. The other parameters are $\alpha = 2.9$, $\beta = 10$, and $N = 100$.

interactions among elements have a nonlocal character. Each lattice element is coupled to all neighbors within a square with the side $2R + 1$ centered on the given element. In the case considered, R is half the square edge; however, for convenience, we use the conventional terminology, calling the normalized quantity $r = R/N$ the coupling radius. Ensemble (15) has $N^2 = 100 \times 100$ elements. The values of parameters α and β in the cubic map were selected to agree with the regime of developed chaos with a unified attractor ($\alpha = 2.9$, $\beta = 10$).

For a fixed parameter $\beta = 10$ and α varying, the cubic map demonstrates different dynamical regimes [159]. For $1 < \alpha < 2.4$, there are two stable fixed points on the map. With α increasing, each of them demonstrates a cascade of period doubling bifurcations leading to the appearance of two chaotic attractors, symmetric relative to $x = 0$. For $\alpha < 2.84$, the cubic map is bistable. The values of x^{t+1} are either only in the positive or only in the negative domain, depending on the choice of initial conditions. The parameter value $\alpha_{cr} = 2.84$ is critical and corresponds to the union or crisis of symmetric chaotic attractors. For $\alpha > \alpha_{cr}$, points at any trajectory belong to a unique chaotic attractor, which reflects bistability in a certain sense [159].

In the case of an ensemble of coupled maps (15), the effective parameter value α_{eff} is variable because of the effect of coupling, which explains the appearance of regular regimes and complex spatial structures in the transition from coherent to incoherent chaos for a decreasing coupling parameter σ [see (11)].

If the coupling strength exceeds the value $\sigma = 0.05$, the behavior of lattice elements becomes bistable with time. Each element can stay in the region of either positive or negative states. However, for arbitrary initial conditions, combined spatial structures are realized: some of the elements oscillate in the region of negative values, and others in the region of positive values. When the coupling parameter reaches the value $\sigma = 0.1$, a transition to the regime of single-well structures occurs. With a further increase in the coupling strength, the correlation between elements increases, leading to the appearance of clusters with fundamentally different behaviors of neighboring elements. Elements of one lattice part behave coherently with respect to each other, whereas elements of the other part behave incoherently. Thus a transition to a chimera state regime occurs. The chimera structures observed are characterized by all lattice elements that are in regions of either positive or negative values. Chimeras analogous to phase and amplitude chimeras found in chains of logistic maps or chaotic autogenerators [75, 91] can be realized.

With an increase in the coupling strength σ, a bifurcation occurs for chimera structures belonging to different attractors (either negative or positive), and a new chimera type emerges, characterized by the elements of coherent clusters being in the vicinity of one attractor, whereas the elements belonging to incoherent clusters are irregularly distributed between the two attractors. Such chimeras cannot occur in systems of coupled oscillators with one attractor. All system elements in this case oscillate within one attractor, never switching over to the other one. This type of chimera was called the *double-well chimera*. An example of such a structure is given in Fig. 14.

We note that the majority of chimeras observed in the lattice are combined ones, i.e., include incoherent clusters characteristic of chimeras of different types: phase, amplitude, and double-well.

10. External and mutual synchronization of chimera states

We explore effects of chimera state synchronizationly resorting to examples of systems of coupled ensembles comprising various oscillators with chaotic dynamics [124, 160]. For clarity, we consider the simplest example of chimera structure synchronization in a system of two coupled ensembles consisting of rings of logistic maps with a nonlocal coupling and misfit in governing parameters. The system equations

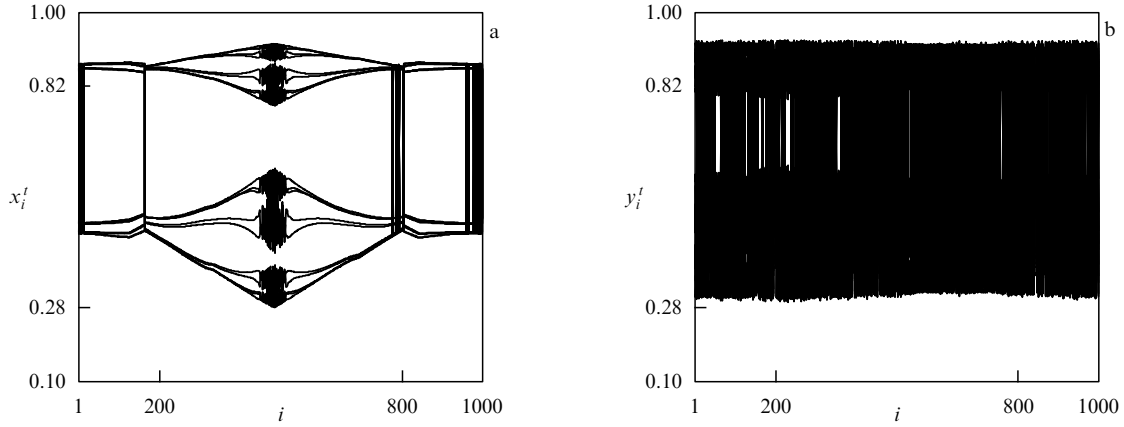

Figure 15. Spatio-temporal profiles of the amplitudes (a) x_i^t in the first ring and (b) y_i^t in the second ring of logistic maps in the absence of coupling between the rings.

have the form

$$
\begin{aligned}
x_i^{t+1} &= f_i^t + \frac{\sigma_1}{2P}\sum_{j=i-P}^{i+P}\left(f_j^t - f_i^t\right) + \gamma_{21}F_i^t,\\
y_i^{t+1} &= g_i^t + \frac{\sigma_2}{2R}\sum_{j=i-R}^{i+R}\left(g_j^t - g_i^t\right) - \gamma_{12}F_i^t,\\
f_i^t &= \alpha_1 x_i^t(1-x_i^t), \qquad g_i^t = \alpha_2 y_i^t(1-y_i^t)\,.
\end{aligned}
\tag{16}
$$

Here, α_1 and α_2 are the nonlinearity parameters of the logistic maps, σ_1 and σ_2 are the nonlocal coupling coefficients, P and R are the numbers of neighbors on both sides of the ith element in the respective first and second rings, $N = 1000$ is the number of elements in each ring, $F_i^t = g_i^t - f_i^t$ is the function of dissipative coupling between the rings, and γ_{21} and γ_{12} are the coefficients of coupling between the rings. In the case of external synchronization, $\gamma_{21} = 0$ and $\gamma_{12} = \gamma$. For the regime of mutual synchronization, $\gamma_{21} = \gamma_{12} = \gamma$.

10.1 External synchronization of spatio-temporal structures

We select the parameters of the first and second rings such that different spatio-temporal structures are established in them in the absence of coupling. We fix parameters that are the same for both rings, $R = P = 320$ and $N = 1000$, and take the values $\alpha_1 = 3.7$, $\sigma_1 = 0.23$ and $\alpha_2 = 3.85$, $\sigma_2 = 0.15$. Figure 15 shows spatio-temporal profiles for amplitudes in the two rings in the absence of coupling. As can be seen, for the selected parameter values, the regime of phase and amplitude chimeras is realized in the first ring x_i^t (Fig. 15a), and a regime close to spatio-temporal chaos is established in the second ring y_i^t (Fig. 15b). The above parameter values are not critical. The main requirement needed to explore the effect of synchronization is that these parameters provide different spatio-temporal structures in the rings without coupling. We note that spatio-temporal profiles that we use to illustrate the dynamics of elements in coupled rings in this section are a set of the last 100 instantaneous profiles of ensemble states (or the last 100 iterations of system (16)).

We now trace the evolution of structures in the second ring when a unidirectional coupling is introduced, i.e., when the first (driving) ring of logistic maps acts on the second (driven) ring, with the coupling coefficients $\gamma_{12} = \gamma$ and $\gamma_{21} = 0$. Computations indicate that after the coupling is introduced, spatial structures in the second ring undergo modifications as γ is increased, gradually approaching the structure in the governing ring (Fig. 15a). If the coupling coefficient reaches the value $\gamma = 0.40$ or higher, the structure in the driven ring acquires a form identical to that in the driving ring. Figure 16 illustrates this evolution.

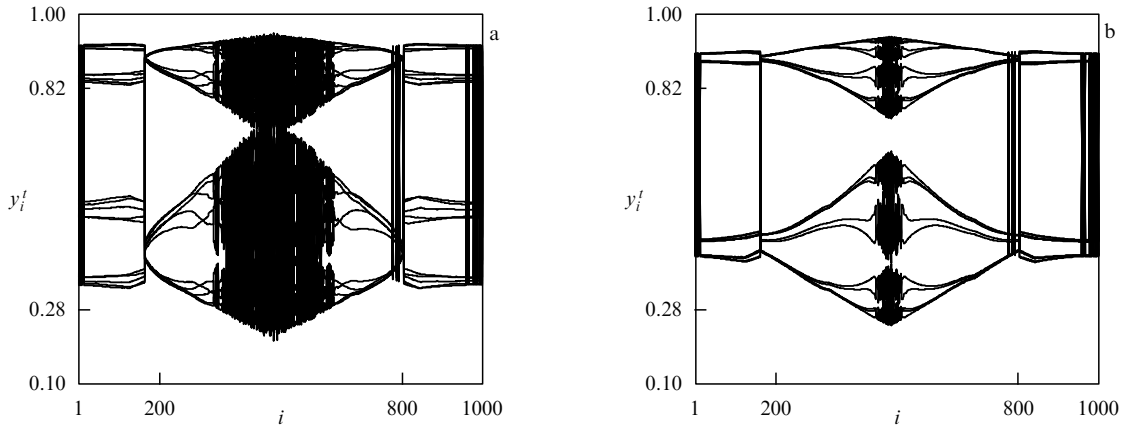

Figure 16. Spatio-temporal profiles of the amplitudes y_i^t in the second ring for (a) $\gamma = 0.15$, when the effect of external synchronization is still absent, and (b) $\gamma = 0.45$, when it is present.

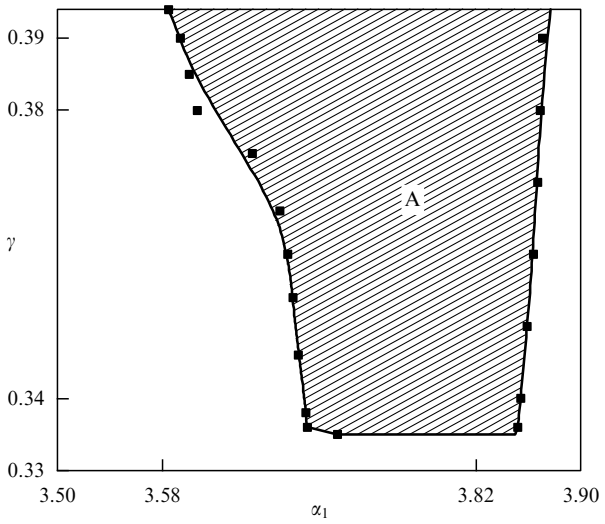

Figure 17. Region of external synchronization of spatio-temporal structures in system (16) in the parameter plane (α_1, γ) for $\alpha_2 = 3.85$, $\sigma_1 = 0.23$, and $\sigma_2 = 0.15$. In hatched domain A, the crosscorrelation coefficient for oscillators x_i^t and y_i^t is $R_i > 0.99$.

To prove that we are dealing with the external synchronization of chimera structures, the results presented in Fig. 16 are, strictly speaking, insufficient. The similarity of synchronous structures has to be quantified and the existence of a finite synchronization domain in the system parameter space must be shown. One possible quantitative characteristic for the synchronous dynamics of two oscillators can be the CC

$$R_i = \frac{\langle \tilde{x}_i(t)\tilde{y}_i(t)\rangle}{\sqrt{\langle \tilde{x}_i^2(t)\rangle \langle \tilde{y}_i^2(t)\rangle}}\,, \qquad (17)$$

$$\tilde{x}_i(t) = x_i(t) - \langle x_i(t)\rangle\,,$$

$$\tilde{y}_i(t) = y_i(t) - \langle y_i(t)\rangle\,,$$

where x_i and y_i are the amplitudes of oscillations in the first and second coupled ensembles, the angular brackets denote time averaging, and $i = 1, 2, \ldots, N$ are the numbers of respective elements in the coupled ensembles. Synchronous dynamics of oscillators would be identified with $R_i = 1$ for all ensemble oscillators, whereas the coefficient R is less than unity if synchronization is absent. Computations showed that the structure given in Fig. 16b is indeed identical, and hence synchronous, to the first structure observed in the driving ring in the absence of coupling between the rings (Fig. 15a). In this case, the CC is $R_i > 0.99$ and this condition is observed for a finite region in the domain of governing parameters. Thus, we can argue that for a unidirected coupling, the chimera structure of the first (driving) ring synchronizes the structure in the second (driven) ring, and the effect of external synchronization is realized for chimera structures.

More revealing is an experiment whose results are shown in Fig. 17. We set $\alpha_2 = 3.85$ in the driven ring and construct the region of synchronization in the plane of two parameters: the coupling coefficient γ and the nonlinearity parameter for the driving ring α_1. Changes in α_1 modify spatio-temporal structures in the driving ring. As follows from computations, the structures that are then realized in the driving ring synchronize like structures in the governed ring as the coupling parameter γ increases. Further, varying the coupling coefficient, we compute the CC R and draw the synchronization domain shown in Fig. 17. In the hatched domain A, the coefficient is $R > 0.99$, implying that in domain A structures are realized that are identical to the structures in the governing ring. It should be kept in mind that under varying α_1 and γ within domain A, the structures observed may vary owing to variations in the parameter α_1 in the driving ring. However, everywhere in domain A the structures of the first and second rings are synchronous. We note that Fig. 17 suggests the existence of a synchronization threshold, which originates from the fact that individual oscillators in ensembles are not identical and from the nonlocality of the coupling.

10.2 Mutual synchronization of spatio-temporal structures

With the goal of exploring mutual synchronization of chimera structures, we add a symmetric bi-directional coupling to Eqn (16) for coupled rings by setting $\gamma_{12} = \gamma_{21} = \gamma$. Introducing a small misfit in the parameters α_1 and α_2 in the ensembles of logistic maps, we create different chimera structures in the first and second rings (Fig. 18a). With the coupling introduced, as follows from computations, the structures start to approach each other, and for $\gamma > 0.07$ the chimera structures become synchronized (Fig. 18c).

Computations of the CC showed that $R > 0.99$ in the synchronization regime and that this condition holds for a finite range of the coupling coefficient. Thus, we can state that mutual synchronization of chimera structures is realized in coupled ensembles (16). We note that synchronous structures do not coincide with the structures in the first and second ensemble without coupling, which is apparent from Fig. 18c.

The details of the synchronization effect for structures of coupled ensembles (16) qualitatively correspond to the classical theory of limit cycle synchronization. This fact allows the results described to be regarded as a generalization of ideas of the classical synchronization theory for periodic auto-oscillations to the case of synchronization of spatio-temporal structures in systems of coupled ensembles of nonlinear oscillators.

11. Conclusions

In this review, we presented the results obtained in studies of different types of spatio-temporal structures realized in ensembles of nonlocally coupled chaotic oscillators with discrete and continuous time. Relatively simple ensembles in the form of a one-dimensional ring of nonlocally coupled oscillators and systems of two coupled ensembles were considered. The main focus was on exploring dynamical and statistical properties of chimera structures characterized by the coexistence of spatially localized clusters with coherent and incoherent dynamics in the ensemble.

We briefly recapitulate the main results. In Section 2, we presented studies of so-called phase chimeras. Computations were carried out using a simple example of a one-dimensional ring of nonlocally coupled logistic maps in the chaotic regime of individual oscillators. It was found that an incoherent cluster of phase chimeras comprises a finite number of ensemble oscillators whose oscillations change their 'phase' irregularly in space. In Section 3, we presented the mechanism of phase chimera formation and its statistical characteristics. In Section 4, we described a new type of chimera structure called the amplitude chimera, reviewing the results of studies exploring the realization mechanism, statistical characteris-

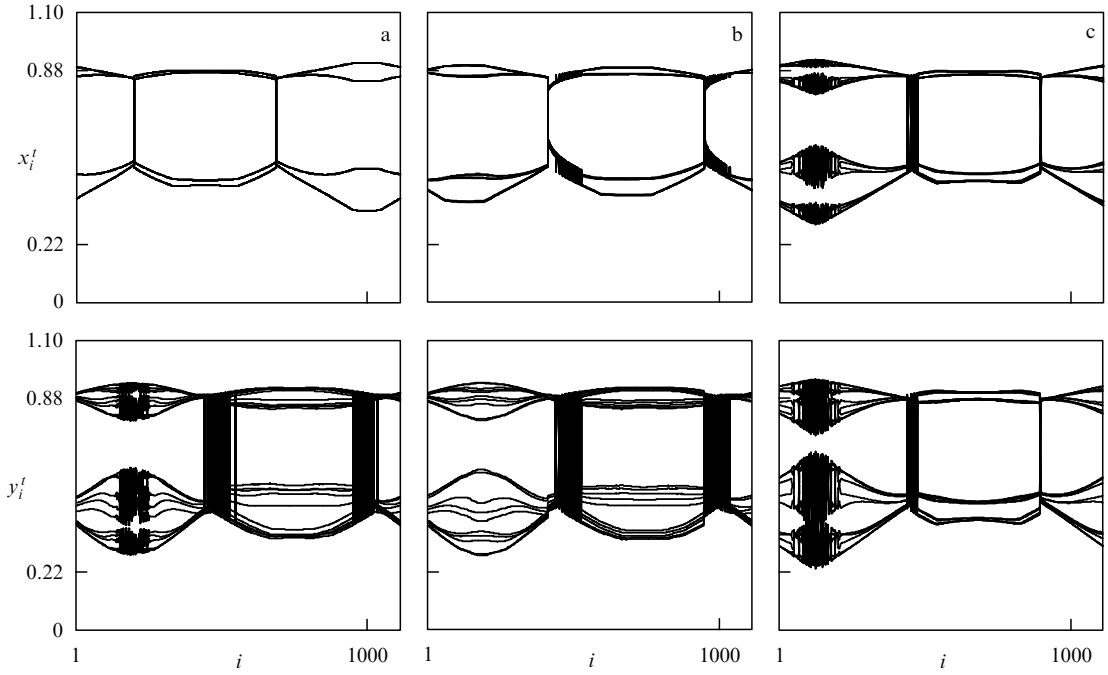

Figure 18. Effect of mutual synchronization of chimera structures in symmetrically coupled ensembles x_i^t (top row) and y_i^t (bottom row) for the coupling parameter γ: (a) 0, (b) 0.025, (c) 0.075 and $\alpha_1 = 3.7$, $\alpha_2 = 3.85$, and $\sigma_1 = \sigma_2 = 0.28$.

tics, and lifetime of amplitude chimera clusters. It was confirmed by numerical simulations that the appearance of phase and amplitude chimera structures is typical for a broad class of ensembles with nonlocal coupling, with individual elements being discrete or differential systems realizing a transition to chaos through a cascade of period doubling bifurcations.

The connection was presented between the types of chimera structures in ensembles of chaotic oscillators and the type of chaotic attractor for an individual oscillator. In Section 5, we presented results indicating that chimera structures occur in ensembles of oscillators with nonhyperbolic attractors and are still not found in ensembles with quasihyperbolic attractors. Based on this, we proposed to use basic models in the form of discrete Hénon and Lozi maps as individual oscillators in ensembles. An ensemble of Hénon elements is a system with a nonhyperbolic attractor, and an ensemble of Lozi elements describes a system with a quasihyperbolic attractor. With the help of these models, it is possible to describe characteristics and properties of spatio-temporal structures for a wide class of ensembles composed of chaotic oscillators. A feature of ensembles with oscillators having a quasihyperbolic type of attractor is the realization of structures containing oscillators with abrupt amplitude spikes (regimes of solitary states). In Section 6, devoted to a description of solitary state regimes, we reported on the results of studies exploring the mechanisms whereby this regime is realized. It was found that the cause of solitary state occurrence is the loss of quasihyperbolicity by the Lozi system and the emergence of the bistable regime. A system of two interacting ensembles of Hénon and Lozi maps was discussed in Section 7. A chimera structure of a new type — the solitary state chimera — was described, whose incoherent cluster includes oscillators in the solitary state regime. In Section 8, we presented original research on mechanisms whereby regimes of solitary states and solitary state chimeras occur in a one-dimensional ring of nonlocally coupled Hénon maps. It was demonstrated that these regimes also originate from the birth of bistability. The results of numerical analysis pertaining to the so-called double-well chimera, which occurs for a wide class of bistable oscillators, were discussed in Section 9. In Section 10, we discussed the effects of external and mutual synchronization of chimera structures in the simplest system of two interacting one-dimensional ensembles of nonlocally coupled logistic maps. These results indicate that details of the effects of external and mutual synchronization of spatio-temporal structures, including chimera states, qualitatively correspond to the classical theory of limit cycle synchronization.

At present, the efforts of numerous researchers are aimed at studying processes leading to the formation of spatio-temporal structures in more complex multi-component systems. Such systems consist of several mutually connected ensembles of various types of nonlinear oscillators with different topologies and types of coupling between the oscillators inside ensembles, as well as between the ensembles. The authors hope that the results presented in this review will be helpful in solving more complex problems.

The authors use this pleasant opportunity to express their deep gratitude to E Schöll and A Zakharova of the Berlin Technical University for the fruitful discussions and collaboration on the set of problems presented in this review. We are also indebted to colleagues in the Department of Radiophysics and Nonlinear Dynamics of Saratov University, T E Vadivasova, N I Semenova, A I Shepelev, A V Bukh, and E V Rybalova, for their contributions and active discussions.

The results presented in this review were obtained under financial support grants from the Russian Foundation of Basic Research, no. 15-02-02288, the Russian Science Foundation, no. 16-12-10175, and the State Assignment of the Ministry of Education and Science of the RF, no. 3.8616.2017/BCh, SFB910.

References

1. Nicolis G, Prigogine I *Self-Organization in Non-Equilibrium Systems: from Dissipative Structures to Order Through Fluctuations* (New York: Wiley, 1977); Translated into Russian: *Samoorganizatsiya v Neravnovesnykh Sistemakh: Ot Dissipativnykh Struktur k Uporyadochennosti cherez Fluktuatsii* (Moscow: Mir, 1979)
2. Landa P S *Avtokolebaniya v Raspredelennykh Sistemakh* (Self-Oscillations in Distributed Systems) (Moscow: Nauka, 1983)
3. Haken H *Synergetics. An Introduction. Nonequilibrium Phase Transitions and Self-Organization in Physics, Chemistry, and Biology* 3rd ed. (Berlin: Springer, 1983)
4. Polak L S, Mikhailov A S *Samoorganizatsiya v Neravnovesnykh Fiziko-Chimicheskikh Sistemakh* (Self-Organization in Nonequilibrium Physicochemical Systems) (Moscow: Nauka, 1983)
5. Kuramoto Y *Chemical Oscillations, Waves and Turbulence* (Berlin: Springer-Verlag, 1984)
6. Vasil'ev V A, Romanovsky Yu M, Yakhno V G *Avtovolnovye Protsessy* (Autowave Processes) (Moscow: Nauka, 1987)
7. Afraimovich V S et al. *Stability, Structures, and Chaos in Nonlinear Synchronization Networks* (World Scientific Series on Nonlinear Science A, Vol. 6, Eds A V Gaponov-Grekhov, M I Rabinovich) (Singapore: World Scientific, 1994); Translated from Russian: *Ustoichivost', Struktury i Khaos v Nelineinykh Setyakh s Sinkhronizatsiei* (Eds A V Gaponov-Grekhov, M I Rabinovich) (Gor'ky: IPF, 1989)
8. Epstein I R, Pojman J A *An Introduction to Nonlinear Chemical Dynamics: Oscillations, Waves, Patterns, and Chaos* (New York: Oxford Univ. Press, 1998)
9. Winfree A T *The Geometry of Biological Time* (New York: Springer, 2001)
10. Pikovsky A, Rosenblum M, Kurths J *Synchronization. A Universal Concept in Nonlinear Sciences* (Cambridge: Cambridge Univ. Press, 2001)
11. Mosekilde E, Maistrenko Yu, Postnov D *Chaotic Synchronization: Applications to Living Systems* (River Edge, NJ: World Scientific, 2002)
12. Nekorkin V I, Velarde M G *Synergetic Phenomena in Active Lattices. Patterns, Waves, Solitons, Chaos* (Berlin: Springer, 2002)
13. Loskutov A Yu, Mikhailov A S *Osnovy Teorii Slozhnykh Sistem* (Fundamentals of the Theory of Complex Systems) (Moscow–Izhevsk: Inst. Komp'yut. Issled., 2007)
14. Malchow H, Petrovskii S V, Venturino E *Spatiotemporal Patterns in Ecology and Epidemiology: Theory, Models, and Simulation* (Boca Raton, FL: Chapman and Hall. CRC Press, 2007)
15. Osipov G V, Kurths J, Zhou C *Synchronization in Oscillatory Networks* (Berlin: Springer, 2007)
16. Jones C K R T *Trans. Am. Math. Soc.* **286** 431 (1984)
17. Waller I, Kapral R *Phys. Rev. A* **30** 2047 (1984)
18. Pertsov A M, Ermakova E A, Panfilov A V *Physica D* **14** 117 (1984)
19. Ermentrout G B, Troy W C *SIAM J. Appl. Math.* **39** 623 (1986)
20. Gaponov-Grekhov A V, Rabinovich M I *Radiophys. Quantum Electron.* **30** 93 (1987); *Izv. Vyssh. Uchebn. Zaved. Radiofiz.* **30** (2) 131 (1987)
21. Sakaguchi H, Shinomoto S, Kuramoto Y *Prog. Theor. Phys.* **77** 1005 (1987)
22. Strogatz S H, Mirollo R E *J. Phys. A* **21** L699 (1988)
23. Strogatz S H, Mirollo R E *Physica D* **31** 143 (1988)
24. Kaneko K *Physica D* **37** 60 (1989)
25. Kaneko K *Physica D* **34** 1 (1989)
26. Kuznetsov A P, Kuznetsov S P *Radiophys. Quantum Electron.* **34** 845 (1991); *Izv. Vyssh. Uchebn. Zaved. Radiofiz.* **34** 1079 (1991)
27. Astakhov V V, Bezruchko B P, Ponomarenko V I *Radiophys. Quantum Electron.* **34** 28 (1991); *Izv. Vyssh. Uchebn. Zaved. Radiofiz.* **34** 35 (1991)
28. Cross M C, Hohenberg P C *Rev. Mod. Phys.* **65** 851 (1993)
29. Nekorkin V I, Makarov V A *Phys. Rev. Lett.* **74** 4819 (1995)
30. Abarbanel H D et al. *Phys. Usp.* **39** 337 (1996); *Usp. Fiz. Nauk* **166** 363 (1996)
31. Nekorkin V I, Kazantsev V B, Velarde M G *Phys. Lett. A* **236** 505 (1997)
32. Nekorkin V I, Voronin M L, Velarde M G *Eur. Phys. J. B* **9** 533 (1999)
33. Belykh V N, Belykh I V, Hasler M *Phys. Rev. E* **62** 6332 (2000)
34. Nagai Y et al. *Phys. Rev. Lett.* **84** 4248 (2000)
35. Belykh V N, Belykh I V, Mosekilde E *Phys. Rev. E* **63** 036216 (2001)
36. Zaritski R M, Pertsov A M *Phys. Rev. E* **66** 066120 (2002)
37. Borisyuk G N et al. *Phys. Usp.* **45** 1073 (2002); *Usp. Fiz. Nauk* **172** 1189 (2002)
38. El'kin Yu E *Matem. Biol. Bioinform.* **1** (1) 27 (2006)
39. Anishchenko V S et al. *New J. Phys.* **8** 84 (2006)
40. Belykh V N et al. *Chaos* **18** 037106 (2008)
41. Shabunin A, Feudel U, Astakhov V *Phys. Rev. E* **80** 026211 (2009)
42. Rosin D P et al. *Phys. Rev. Lett.* **110** 104102 (2013)
43. Motter A E et al. *Nature Phys.* **9** 191 (2013)
44. Klinshov V V, Nekorkin V I *Phys. Usp.* **56** 1217 (2013); *Usp. Fiz. Nauk* **183** 1323 (2013)
45. Pecora L M et al. *Nature Commun.* **5** 4079 (2014)
46. Maslennikov O V, Nekorkin V I *Phys. Usp.* **60** 694 (2017); *Usp. Fiz. Nauk* **187** 745 (2017)
47. Kuramoto Y, Battogtokh D *Nonlin. Phenomena Complex Syst.* **5** 380 (2002)
48. Abrams D M, Strogatz S H *Phys. Rev. Lett.* **93** 174102 (2004)
49. Abrams D M et al. *Phys. Rev. Lett.* **101** 084103 (2008)
50. Laing C R *Phys. Rev. E* **81** 066221 (2010)
51. Laing C R *Physica D* **240** 1960 (2011)
52. Martens E A, Laing C R, Strogatz S H *Phys. Rev. Lett.* **104** 044101 (2010)
53. Motter A E *Nature Phys.* **6** 164 (2010)
54. Wolfrum M, Omel'chenko O E *Phys. Rev. E* **84** 015201(R) (2011)
55. Omelchenko I et al. *Phys. Rev. Lett.* **106** 234102 (2011)
56. Omelchenko I et al. *Phys. Rev. E* **85** 026212 (2012)
57. Omelchenko I et al. *Phys. Rev. Lett.* **110** 224102 (2013)
58. Rosin D P, Rontani D, Gauthier D J *Phys. Rev. E* **89** 042907 (2014)
59. Maistrenko Yu L et al. *Int. J. Bifurcat. Chaos* **24** 1440014 (2014)
60. Zakharova A, Kapeller M, Schöll E *Phys. Rev. Lett.* **112** 154101 (2014)
61. Yeldesbay A, Pikovsky A, Rosenblum M *Phys. Rev. Lett.* **112** 144103 (2014)
62. Sethia G C, Sen A *Phys. Rev. Lett.* **112** 144101 (2014)
63. Böhm F et al. *Phys. Rev. E* **91** 040901(R) (2015)
64. Dudkowski D, Maistrenko Yu, Kapitaniak T *Phys. Rev. E* **90** 032920 (2014)
65. Panaggio M J, Abrams D M *Nonlinearity* **28** R67 (2015)
66. Semenova N et al. *Europhys. Lett.* **112** 40002 (2015)
67. Omelchenko I et al. *Phys. Rev. E* **91** 022917 (2015)
68. Maistrenko Yu et al. *New J. Phys.* **17** 073037 (2015)
69. Olmi S et al. *Phys. Rev. E* **92** 030901(R) (2015)
70. Hizanidis J et al. *Phys. Rev. E* **92** 012915 (2015)
71. Santos M S et al. *Phys. Lett. A* **379** 2188 (2015)
72. Laing C R *Phys. Rev. E* **92** 050904(R) (2015)
73. Clerc M G et al. *Phys. Rev. E* **93** 052204 (2016)
74. Hizanidis J, Lazarides N, Tsironis G P *Phys. Rev. E* **94** 032219 (2016)
75. Bogomolov et al. *Tech. Phys. Lett.* **42** 765 (2016); *Pis'ma Zh. Tekh. Fiz.* **42** (14) 103 (2016)
76. Semenova N I, Anishchenko V S *Nelin. Din.* **12** 295 (2016)
77. Vadivasova T E et al. *Chaos* **26** 093108 (2016)
78. Kemeth F P et al. *Chaos* **26** 094815 (2016)
79. Ulonska S et al. *Chaos* **26** 094825 (2016)
80. Semenova N et al. *Phys. Rev. Lett.* **117** 014102 (2016)
81. Schöll E *Eur. Phys. J. Spec. Top.* **225** 891 (2016)
82. Semenov V et al. *Europhys. Lett.* **115** 10005 (2016)
83. Banerjee T et al. *Phys. Rev. E* **94** 032206 (2016)
84. Sawicki J et al. *Eur. Phys. J. Spec. Top.* **226** 1883 (2017)
85. Tsigkri-DeSmedt N D et al. *Eur. Phys. J. B* **90** 139 (2017)
86. Vadivasova T E et al. *Tech. Phys. Lett.* **43** 118 (2017); *Pis'ma Zh. Tekh. Fiz.* **43** (2) 68 (2017)
87. Semenova N I et al. *Regul. Chaot. Dyn.* **22** 148 (2017)
88. Rybalova E et al. *Eur. Phys. J. Spec. Top.* **226** 1857 (2017)
89. Shepelev I A et al. *Phys. Lett. A* **381** 1398 (2017)
90. Semenova N I et al. *Chaos* **27** 061102 (2017)
91. Bogomolov S A et al. *Commun. Nonlin. Sci. Numer. Simul.* **43** 25 (2017)
92. Shepelev I A, Zakharova A, Vadivasova T E *Commun. Nonlin. Sci. Numer. Simul.* **44** 277 (2017)

93. Shepelev I A et al. *Nonlin. Dyn.* **90** 2317 (2017)
94. Zakharova A et al. *Chaos* **27** 114320 (2017)
95. Shepelev I A, Vadivasova T E *Phys. Lett. A* **382** 690 (2018)
96. Shepelev I A et al. *Commun. Nonlin. Sci. Numer. Simul.* **54** 50 (2018)
97. Shepelev I A, Strelkova G I, Anishchenko V S *Chaos* **28** 063119 (2018)
98. Bukh A V et al. *Regul. Chaot. Dyn.* **23** 325 (2018)
99. Hagerstrom A M et al. *Nature Phys.* **8** 658 (2012)
100. Tinsley M R, Nkomo S, Showalter K *Nature Phys.* **8** 662 (2012)
101. Nkomo S, Tinsley M R, Schowalter K *Phys. Rev. Lett.* **110** 244102 (2013)
102. Larger L, Penkovsky B, Maistrenko Yu *Phys. Rev. Lett.* **111** 054103 (2013)
103. Martens E A et al. *Proc. Natl. Acad. Sci. USA* **110** 10563 (2013)
104. Kapitaniak T et al. *Sci. Rep.* **4** 6379 (2014)
105. Larger L, Penkovsky B, Maistrenko Yu *Nature Commun.* **6** 7752 (2015)
106. Hart J D et al. *Chaos* **26** 094801 (2016)
107. Ponomarenko V I, Kulminskiy D D, Prokhorov M D *Phys. Rev. E* **96** 022209 (2017)
108. Kasimatis T, Hizanidis J, Provata A *Phys. Rev. E* **97** 052213 (2018)
109. Rattenborg N C, Amlaner C J, Lima S L *Neurosci. Biobehavior. Rev.* **24** 817 (2000)
110. Rattenborg N C et al. *Nature Commun.* **7** 12468 (2016)
111. Rothkegel A, Lehnertz K *New J. Phys.* **16** 055006 (2014)
112. Andrzejak R G et al. *Sci. Rep.* **6** 23000 (2016)
113. Laing C R, Chow C C *Neural Comput.* **13** 1473 (2001)
114. Sakaguchi H *Phys. Rev. E* **73** 031907 (2006)
115. Hizanidis J et al. *Sci. Rep.* **6** 19845 (2016)
116. Davidenko J M et al. *Nature* **355** 349 (1992)
117. Cherry E M, Fenton F H *New J. Phys.* **10** 125016 (2008)
118. Motter A E et al. *Nature Phys.* **9** 191 (2013)
119. Nishikawa T, Motter A E *New J. Phys.* **17** 015012 (2015)
120. Martens E A, Klemm K *Front. Phys.* **6** 62 (2017)
121. Shepelev I A et al. *Nonlinear Dyn.* **94** 1019 (2018)
122. Boccaletti S et al. *Phys. Rep.* **544** 1 (2014)
123. Andrzejak R G, Ruzzene G, Malvestio I *Chaos* **27** 053114 (2017)
124. Bukh A et al. *Chaos* **27** 111102 (2017)
125. Sharkovsky A N et al. *Dynamics of One-Dimensional Maps* (Boston: Kluwer Acad. Publ., 1997); Translated from Russian: *Dinamika Odnomernykh Otobrazhenii* (Kiev: Nauk. Dumka, 1989)
126. May R M *Nature* **261** 459 (1976)
127. Rössler O E *Phys. Lett. A* **57** 397 (1976)
128. Anishchenko V S *Slozhnye Kolebaniya v Prostykh Sistemakh* (Complex Oscillations in Simple Systems) 2nd ed. (Moscow: Libkorom, 2009)
129. Anishchenko V S, Vadivasova T E *Lektsii po Nelineinoi Dinamike* (Lectures on Nonlinear Dynamics) (Moscow–Izhevsk: RKhD, 2011)
130. Madan R N (Ed.) *Chua's Circuit*: *A Paradigm for Chaos* (Singapore: World Scientific, 1993)
131. Dziubak V, Maistrenko Yu, Schöll E *Phys. Rev. E* **87** 032907 (2013)
132. Lorenz E N *J. Atmos. Sci.* **20** 130 (1963)
133. Lorenz E N, in *Strannye Attraktory* (Strange Attractors) (Eds Ya G Sinai, L P Shil'nikov) (Moscow: Mir, 1981) p. 88, Translated into Russian [132]
134. Afraimovich V S, Bykov V V, Shil'nikov L P *Sov. Phys. Dokl.* **22** 253 (1977); *Dokl. Akad. Nauk SSSR* **234** 336 (1977)
135. Shilnikov L P, in *The Hopf Bifurcation and Its Applications* (Applied Mathematical Sciences, Vol. 19, Eds J E Marsden, M McCracken) (New York: Springer-Verlag, 1976); Translated into Russian: in *Bifurkatsiya Rozhdeniya Tsikla i ee Prilozheniya* (Eds J E Marsden, M McCracken) (Moscow: Mir, 1980) p. 317
136. Feigenbaum M J *J. Stat. Phys.* **19** 25 (1978)
137. Kuznetsov S P *Phys. Usp.* **54** 119 (2011); *Usp. Fiz. Nauk* **181** 121 (2011)
138. Afraimovich V S, Shilnikov L P, in *Nonlinear Dynamics and Turbulence* (Eds G I Barenblatt, G Iooss, D D Joseph) (Boston: Pitman, 1983) p. 1
139. Shilnikov L *Int. J. Bifurc. Chaos* **07** 1953 (1997)
140. Hénon M *Commun. Math. Phys.* **50** (1) 69 (1976); Translated into Russian: in *Strannye Attraktory* (Strange Attractors) (Eds Ya G Sinai, L P Shilnikov) (Moscow: Mir, 1981) p. 152
141. Lozi R *J. Phys. Colloques* **39** (C5) C5-9 (1978)
142. Shilnikov L P, in *Metody Kachestvennoi Teorii Differentsial'nykh Uravnenii* (Methods of the Qualitative Theory of Differential Equations) (Exec. Ed. E A Leontovich-Andronov) (Gor'ky: GGU, 1986) p. 150
143. Gavrilov N K, Šil'nikov L P *Math. USSR-Sbornik* **17** 467 (1972); Gavrilov N K, Shilnikov L P *Matem. Sb.* **88** 475 (1972)
144. Gavrilov N K, Šil'nikov L P *Math. USSR-Sbornik* **19** 139 (1973); Gavrilov N K, Shilnikov L P *Matem. Sb.* **90** 139 (1973)
145. Bykov V V, Shilnikov L P, in *Metody Kachestvennoi Teorii i Teoriya Bifurkatsii* (Qualitative Theory Methods and Bifurcation Theory) (Exec. Ed. L P Shil'nikov) (Gor'ky: GGU, 1989) p. 151
146. Rybalova E V, Strelkova G I, Anishchenko V S *Chaos Solitons Fractals* **115** 300 (2018)
147. Ashwin P, Buescu J, Stewart I *Nonlinearity* **9** 703 (1996)
148. Ott E, Sommerer J C *Phys. Lett. A* **188** 39 (1994)
149. Hasler M, Maistrenko Y L *IEEE Trans. Circuits Syst. I* **44** 856 (1997)
150. Gibbs H M *Optical Bistability*: *Controlling Light with Light* (Orlando: Academic Press, 1985)
151. Hänggi P, Talkner P, Borkovec M *Rev. Mod. Phys.* **62** 251 (1990)
152. Schlögl F *Z. Phys.* **253** 147 (1972)
153. Goldbeter A *Biochemical Oscillations and Cellular Rhythms* (Cambridge: Cambridge Univ. Press, 1996)
154. Izhikevich E M *Dynamical Systems in Neuroscience. The Geometry of Excitability and Bursting* (Cambridge: MIT Press, 2007)
155. May R M *Nature* **269** 471 (1977)
156. Benzi R, Sutera A, Vulpiani A *J. Phys. A* **14** L453 (1981)
157. Guttal V, Jayaprakash C *Ecol. Model.* **201** 420 (2007)
158. Benzi R *Nonlin. Processes Geophys.* **17** 431 (2010)
159. Skjolding H et al. *SIAM J. Appl. Math.* **43** 520 (1983)
160. Bukh A V, Strelkova G I, Anishchenko V S *Russ. J. Nonlin. Dyn.* **14** 419 (2018)